AMERICAN SOCIETY FOR MICROBIOLOGY | Infection and Immunity®

BACTERIAL INFECTIONS

The Pathogenic Potential of *Proteus mirabilis* Is Enhanced by Other Uropathogens during Polymicrobial Urinary Tract Infection

Chelsie E. Armbruster,[a] Sara N. Smith,[a] Alexandra O. Johnson,[a] Valerie DeOrnellas,[a] Kathryn A. Eaton,[b] Alejandra Yep,[c] Lona Mody,[d,e] Weisheng Wu,[f] Harry L. T. Mobley[a]

Department of Microbiology and Immunology, University of Michigan Medical School, Ann Arbor, Michigan, USA[a]; Laboratory Animal Medicine Unit, University of Michigan Medical School, Ann Arbor, Michigan, USA[b]; Biological Sciences Department, California Polytechnic State University, San Luis Obispo, California, USA[c]; Division of Geriatric and Palliative Medicine, University of Michigan Medical School, Ann Arbor, Michigan, USA[d]; Geriatrics Research Education and Clinical Center, VA Ann Arbor Healthcare System, Ann Arbor, Michigan, USA[e]; Department of Computational Medicine & Bioinformatics, University of Michigan Medical School, Ann Arbor, Michigan, USA[f]

ABSTRACT Urinary catheter use is prevalent in health care settings, and polymicrobial colonization by urease-positive organisms, such as *Proteus mirabilis* and *Providencia stuartii*, commonly occurs with long-term catheterization. We previously demonstrated that coinfection with *P. mirabilis* and *P. stuartii* increased overall urease activity *in vitro* and disease severity in a model of urinary tract infection (UTI). In this study, we expanded these findings to a murine model of catheter-associated UTI (CAUTI), delineated the contribution of enhanced urease activity to coinfection pathogenesis, and screened for enhanced urease activity with other common CAUTI pathogens. In the UTI model, mice coinfected with the two species exhibited higher urine pH values, urolithiasis, bacteremia, and more pronounced tissue damage and inflammation compared to the findings for mice infected with a single species, despite having a similar bacterial burden within the urinary tract. The presence of *P. stuartii*, regardless of urease production by this organism, was sufficient to enhance *P. mirabilis* urease activity and increase disease severity, and enhanced urease activity was the predominant factor driving tissue damage and the dissemination of both organisms to the bloodstream during coinfection. These findings were largely recapitulated in the CAUTI model. Other uropathogens also enhanced *P. mirabilis* urease activity *in vitro*, including recent clinical isolates of *Escherichia coli*, *Enterococcus faecalis*, *Klebsiella pneumoniae*, and *Pseudomonas aeruginosa*. We therefore conclude that the underlying mechanism of enhanced urease activity may represent a widespread target for limiting the detrimental consequences of polymicrobial catheter colonization, particularly by *P. mirabilis* and other urease-positive bacteria.

KEYWORDS CAUTI, *Enterococcus*, *Proteus mirabilis*, *Providencia stuartii*, UTI, catheter-associated urinary tract infection, polymicrobial, urease, urinary tract infection

Urinary catheters are common in health care settings and are utilized by over 60% of critically ill patients, 20% of patients in medical and surgical units, and 5 to 10% of residents in nursing homes (1–3). The incidence of bacteria in urine (bacteriuria) is 3 to 8% per day of catheterization, and long-term catheterization (>30 days) results in continuous bacteriuria (1). The microbial composition of urine colonization changes over time, initially involving *Escherichia coli*, *Klebsiella pneumoniae*, *Serratia* spp., *Citrobacter* spp., *Enterobacter* spp., *Pseudomonas aeruginosa*, and/or Gram-positive cocci and

Received 21 September 2016 **Returned for modification** 13 October 2016 **Accepted** 20 November 2016

Accepted manuscript posted online 28 November 2016

Citation Armbruster CE, Smith SN, Johnson AO, DeOrnellas V, Eaton KA, Yep A, Mody L, Wu W, Mobley HLT. 2017. The pathogenic potential of *Proteus mirabilis* is enhanced by other uropathogens during polymicrobial urinary tract infection. Infect Immun 85:e00808-16. https://doi.org/10.1128/IAI.00808-16.

Editor Shelley M. Payne, University of Texas at Austin

Address correspondence to Chelsie E. Armbruster, chelarmb@umich.edu, or Harry L. T. Mobley, hmobley@umich.edu.

then transitioning to polymicrobial bacteriuria involving urease-positive organisms, including *Proteus mirabilis*, *Providencia stuartii*, and *Morganella morganii* during long-term colonization (1, 4). Up to 50% of individuals catheterized for ≥7 days develop a catheter-associated urinary tract infection (CAUTI), and essentially all individuals catheterized long term experience at least one episode of CAUTI (1).

Historically, the Gram-negative bacterium *P. mirabilis* has been the predominant organism in up to 44% of CAUTIs, particularly with long-term catheterization (4–8). Indeed, we recently determined that *P. mirabilis* was the most common organism in CAUTIs experienced by nursing home residents in southeast Michigan, being present in 48 out of 182 cases (26%) (8). *P. mirabilis* possesses a urea-inducible urease enzyme that hydrolyzes the urea in urine to carbon dioxide and ammonia, providing the bacterium with an abundant nitrogen source while, consequently, increasing urine pH, facilitating the precipitation of polyvalent ions in urine, and resulting in the formation of struvite and apatite crystals (9–11). Several other common uropathogens are urease positive, including *P. stuartii*, *M. morganii*, *Staphylococcus aureus*, and some isolates of *K. pneumoniae* and *P. aeruginosa* (12). Experimentally, however, the urease activity from these organisms is not as potent as that from *P. mirabilis* and therefore is not often associated with the formation of urinary stones (13), while infections with *P. mirabilis* are typically complicated by the formation of bladder and kidney stones and permanent renal damage (9, 14, 15). Notably, we also determined that 57 out of 182 recent CAUTIs (31%) were polymicrobial and *P. mirabilis* was present in 20 of the polymicrobial cases (35%) (8). Thus, *P. mirabilis* is an important CAUTI pathogen to study, particularly in the context of polymicrobial infection.

CAUTI is also the most common source of bacteremia in nursing homes, and the mortality rate is estimated to be as high as 10 to 13% (1, 16). Often, bacteremia is polymicrobial in patients with long-term catheterization (1, 17, 18), and the mortality rate for polymicrobial bacteremia remains high (18, 19). Bacteremia involving *P. mirabilis* more frequently occurs with urinary tract infection (UTI) than other sources of infection (19, 20), and one study reported that 25% of cases of *P. mirabilis* bacteremia were polymicrobial (19), suggesting that interactions between *P. mirabilis* and other uropathogens within the urinary tract may promote progression to bacteremia.

Using an experimental mouse model of ascending UTI, we previously showed that cocolonization with *P. mirabilis* and *P. stuartii* enhances total urease activity and increases disease severity, including an increased incidence of bacteremia and urolithiasis (21). In this study, we expanded on our previous findings to include assessment of disease severity following coinfection in a murine model of CAUTI, utilized urease mutants of both species to delineate the role of enhanced urease activity in the pathogenesis of coinfection, and screened for enhanced urease activity during coculture with recent CAUTI clinical isolates, including vancomycin-resistant *Enterococcus faecalis*. Our results indicate that polymicrobial bacteriuria involving *P. mirabilis* has a deleterious impact on disease progression by promoting an overall increase in urease activity and urine pH, induction of the innate immune response, and tissue damage. The combined result of these effects during polymicrobial infection is an increased likelihood of bacteremia and severe disease.

RESULTS

***Proteus mirabilis* urease activity is enhanced by *Providencia stuartii*.** No urease-positive *Providencia stuartii* genome sequences were available at the start of this study. We therefore sequenced the genome of the multidrug-resistant *P. stuartii* strain BE2467 to verify the urease operon location and orientation and inform our efforts at mutagenesis. Sequencing via the Pacific Biosciences platform resulted in one main chromosome of 4.374 Mb containing 4,212 coding sequences with a 41.4% GC content (GenBank accession number CP017054), a 195,378-nucleotide plasmid containing 255 coding sequences with a 50.7% GC content (GenBank accession number CP017055), and a 38,206-nucleotide plasmid containing 55 coding sequences with a 39.9% GC content (GenBank accession number CP017056). The urease operon of *P. stuartii* BE2467 was

carried only by the larger plasmid, which carries the genes for numerous transferable traits, including sucrose utilization, aminoglycoside resistance via *aphA1*, arsenic resistance, and mercury resistance, along with multiple transposable elements.

Efforts to generate a urease-negative mutant of *P. stuartii* BE2467 by homologous recombination proved unsuccessful. However, a urease-negative mutant of *P. stuartii* was isolated during attempted transposon mutagenesis. For simplicity, this mutant is referred to throughout as *P. stuartii* Δ*ure*, as it was negative for urease activity *in vitro* at all time points tested (Fig. 1A). A *P. mirabilis* mutant with a transposon insertion into the *ureF* gene, resulting in catalytically inactive urease, was used in our prior study (21). This mutant was similarly negative for urease activity *in vitro* at all time points tested (Fig. 1A) and is referred to throughout as *P. mirabilis* Δ*ure*. As previously observed (21), coculture of wild-type (WT) *P. mirabilis* and *P. stuartii* significantly enhanced total urease activity compared to that achieved with a 50:50 mixture of cultures of each species at each time point, and *P. mirabilis* urease activity was required for the enhancement (Fig. 1B and C). However, enhanced activity was not dependent on *P. stuartii* urease activity, as coculture of WT *P. mirabilis* with *P. stuartii* Δ*ure* still resulted in significantly enhanced urease activity compared to that achieved with the 50:50 mixture (Fig. 1D). Thus, interaction with *P. stuartii* enhances *P. mirabilis* urease activity *in vitro* independently of *P. stuartii* urease activity.

To determine if the urease activity within the urinary tract is enhanced during experimental coinfection, female CBA/J mice were transurethrally inoculated with 1×10^7 CFU of *P. mirabilis*, *P. mirabilis* Δ*ure*, *P. stuartii*, or *P. stuartii* Δ*ure* or 1:1 mixtures containing 5×10^6 CFU of each species to maintain the same total inoculum for establishing an ascending UTI. Urine was collected at 6, 24, 48, 72, and 96 h postinoculation (hpi) to determine the pH and bacterial burden. Infection with WT *P. mirabilis* resulted in significantly higher urine pH values than infection with *P. stuartii* or the urease mutants (Fig. 2A). As early as 24 hpi, coinfection with WT *P. mirabilis* and WT *P. stuartii* resulted in significantly higher urine pH values than infection with any single species, suggesting that urease activity is enhanced *in vivo* during experimental coinfection. In comparing coinfection groups, coinfection with both WT isolates resulted in the highest urine pH values overall (Fig. 2B). Notably, at 24 and 48 hpi, mice coinfected with WT *P. mirabilis* and *P. stuartii* Δ*ure* had urine pH values similar to those of mice coinfected with the WT isolates, indicating that *P. stuartii* urease activity is not required to enhance *P. mirabilis* urease activity *in vivo* during experimental UTI at these time points. The urine colonization density varied between mice, and infections involving urease-negative strains tended to have the lowest levels of colonization overall; however, there were no significant differences in the dynamics of urine colonization between infection groups during the 4-day time course (data not shown). Therefore, urease activity is enhanced during experimental coinfection and at earlier time points results in urine pH values significantly higher than those in the other infection groups.

Enhanced urease activity promotes urolithiasis and bacteremia during ascending UTI. We previously determined that coinfection with *P. mirabilis* and *P. stuartii* increased the incidence of bacteremia and urolithiasis during experimental UTI, and both of these consequences of coinfection required *P. mirabilis* urease (21). As enhanced urease activity during coculture *in vitro* and at early time points *in vivo* was not dependent on *P. stuartii* urease, we sought to determine the contribution of *P. stuartii* urease to both urolithiasis and bacteremia at 4 days (96 h) postinoculation. The accumulation of urinary tract pathogens in the spleen is generally accepted to be the result of at least transient bacteremia. Thus, for the purposes of this study, as in our prior study (21), bacteremia refers to the isolation of bacteria from the spleen.

Urease represents an important fitness factor in ascending UTI for both *P. mirabilis* and *P. stuartii*, as infection with urease mutants of either species resulted in a trend toward decreased urine colonization (Fig. 3A) and significantly decreased bladder and kidney colonization (Fig. 3B and C) compared to the levels of colonization achieved by their respective parental isolates. Consistent with the findings of our previous study (21), all coinfection groups exhibited a total bacterial burden in each organ similar to

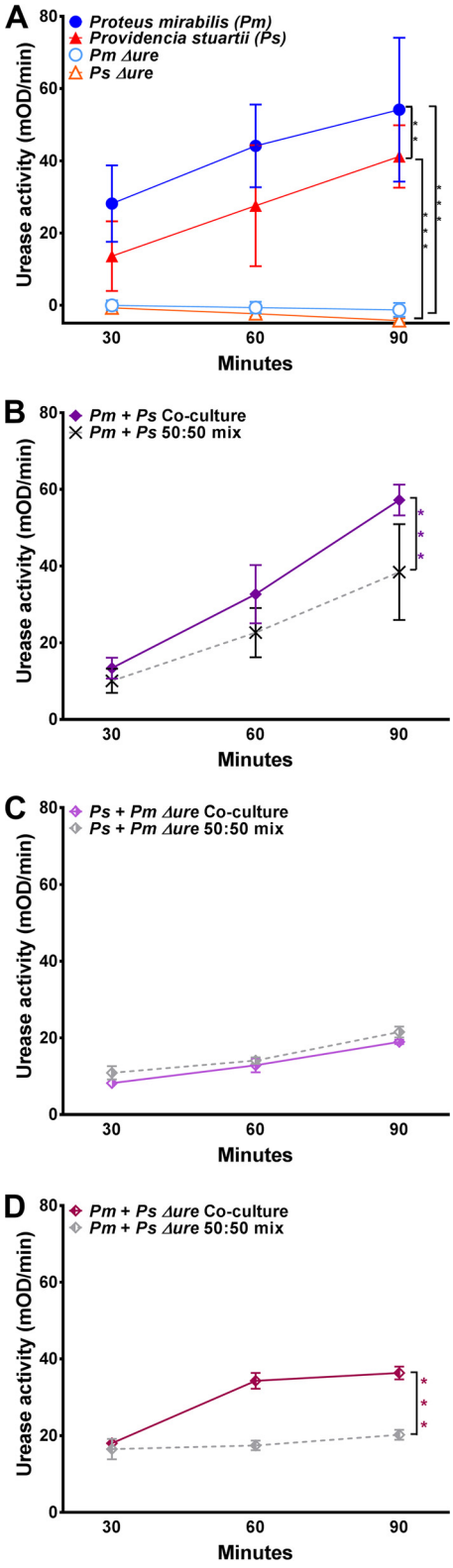

FIG 1 *Providencia stuartii* enhances *Proteus mirabilis* urease activity *in vitro*. (A to D) *P. mirabilis*, *P. stuartii*, and urease mutants were cultured in filter-sterilized human urine to measure urease activity, expressed as the mean change in the optical density per minute (mOD/min) of the indicator dye phenol red during a 5-min kinetic read (see Materials and Methods). (A) Urease activity of *P. mirabilis*, *P. stuartii*, and their respective urease mutants from single-species cultures. (B) Urease activity resulting from coculture of WT *P. mirabilis* with WT *P. stuartii* compared to that resulting from a 50:50 mixture of single-species cultures at each time point. (C) Urease activity resulting from coculture of *P. mirabilis* Δ*ure* with WT *P. stuartii*

(Continued on next page)

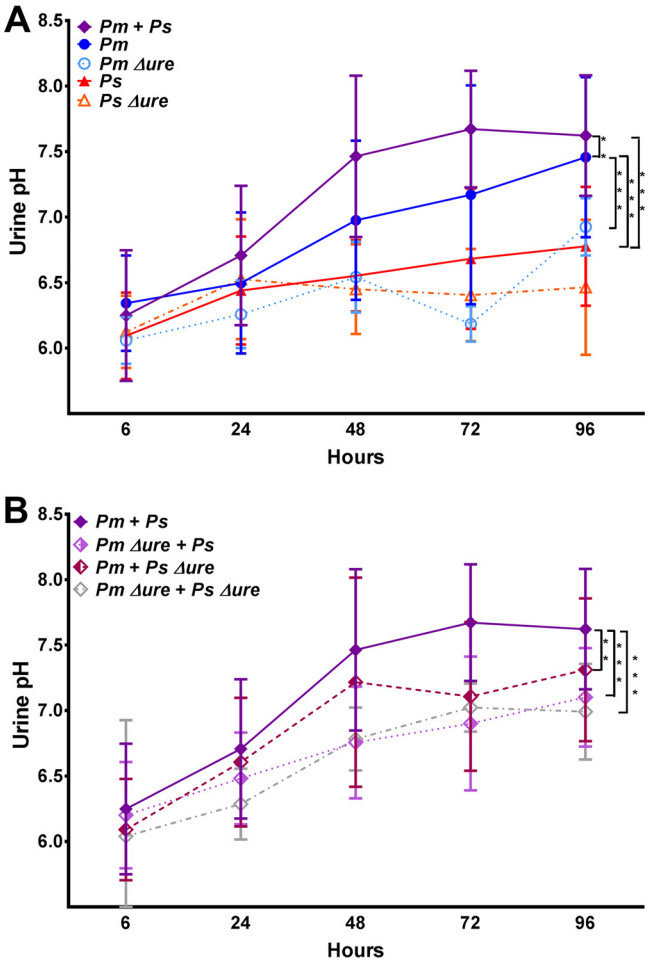

FIG 2 *Providencia stuartii* enhances *Proteus mirabilis* urease activity *in vivo* during polymicrobial infection. CBA/J mice were inoculated transurethrally with 50 μl of 2 $\times$ 10^8 CFU/ml (1 $\times$ 10^7 CFU/mouse) of *P. mirabilis*, *P. stuartii*, or their respective urease mutants or coinfected with 50 μl of a 1:1 mixture of both species containing a total of 2 $\times$ 10^8 CFU/ml (1 $\times$ 10^7 CFU/mouse). Urine was collected at 6, 24, 48, 72, and 96 hpi for pH measurement. (A) Urine pH for mice inoculated with *P. mirabilis*, *P. stuartii*, *P. mirabilis* Δ*ure*, or *P. stuartii* Δ*ure* or coinfected with WT *P. mirabilis* and WT *P. stuartii*. (B) Urine pH for mice coinfected with WT *P. mirabilis* and WT *P. stuartii* compared to that for mice coinfected with either urease mutant. Error bars represent means ± SDs from a minimum of two independent experiments with at least five mice per infection group (total number of mice, 11 to 23 per infection group). *P* values were determined by two-way ANOVA. **, $P < 0.01$; ***, $P < 0.001$.

that exhibited by the groups infected with a single species (Fig. 3). Coinfection with both urease mutants significantly reduced the level of urine and bladder colonization (Fig. 3A and B) compared to that achieved by coinfection with both WT strains, but no significant differences were observed for coinfections in which at least one bacterial species was urease positive. To determine if coinfection resulted in a significant advantage or disadvantage to either species, a coinfection index was calculated as previously described (see Fig. S1 in the supplemental material) (21). Coinfection with WT *P. stuartii* provided a modest advantage to WT *P. mirabilis* in urine (Fig. S1A), coinfection with WT *P. mirabilis* provided an advantage to *P. stuartii* Δ*ure* in the kidneys

FIG 1 Legend (Continued)
compared to that resulting from a 50:50 mixture of single-species cultures at each time point. (D) Urease activity resulting from coculture of WT *P. mirabilis* with *P. stuartii* Δ*ure* compared to that resulting from a 50:50 mixture of single-species cultures at each time point. The graphs are representative of those from at least three independent experiments. Error bars represent means ± standard deviations (SDs) from at least three technical replicates. *P* values were determined by two-way ANOVA. **, $P < 0.01$; ***, $P < 0.001$.

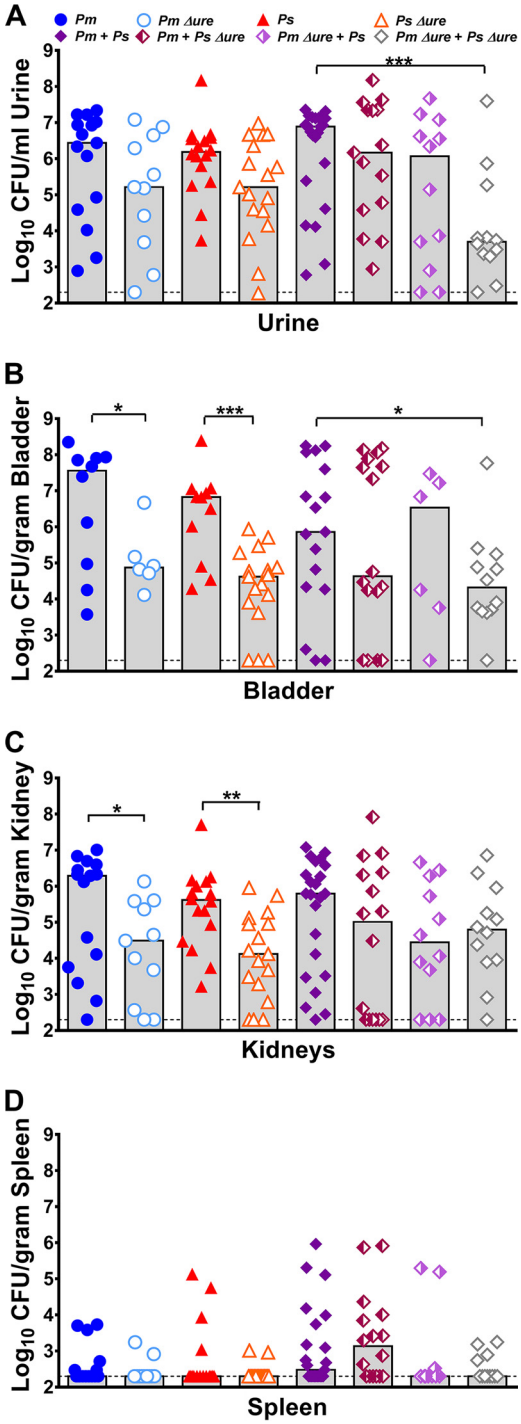

FIG 3 Enhanced urease activity during coinfection increases the incidence of bacteremia but not the bacterial burden within the urinary tract. CBA/J mice were inoculated transurethrally with 50 μl of 2×10^8 CFU/ml (1×10^7 CFU/mouse) of *P. mirabilis*, *P. stuartii*, or their respective urease mutants or coinfected with 50 μl of a 1:1 mixture of both species containing a total of 2×10^8 CFU/ml (1×10^7 CFU/mouse). Urine was collected, and mice were sacrificed at 4 dpi. One-half of the bladder, one-half of each kidney, and the entire spleen were homogenized and plated on LB agar to quantitatively determine the bacterial burden. Each symbol represents the number of CFU per milliliter of urine (A), the number of CFU per gram of bladder tissue (B), the number of CFU per gram of kidney tissue (C), or the number of CFU per gram of spleen tissue from individual mice. Gray bars, median from a minimum of two independent experiments with 5 to 6 mice per infection group (total number of mice, 11 to 23 per infection group); dashed lines, limit of detection. *P* values were determined by a nonparametric Mann-Whitney test. *, $P < 0.05$; **, $P < 0.01$; ***, $P < 0.001$.

(Fig. S1C), and coinfection with *P. stuartii* Δ*ure* provided a modest advantage to *P. mirabilis* Δ*ure* in urine (Fig. S1A).

By the nonparametric Mann-Whitney test, no individual infection group significantly altered the spleen bacterial burden (Fig. 3D). However, in a logistic regression model, coinfections resulted in a significant increase in the percentage of mice that developed bacteremia compared to the findings obtained with single-species infections (odds ratio [OR] = 2.5 [95% confidence interval {CI} = 1.2 to 5.4]; $P < 0.015$). As shown in Table 1, mice with coinfections that had enhanced urease activity *in vitro* (WT *P. mirabilis* with WT *P. stuartii* and WT *P. mirabilis* with *P. stuartii* Δ*ure*) had the highest incidence of urolithiasis and had significantly more bacteremia than mice in the other coinfection groups (OR = 3.3 [95% CI = 1.2 to 9.2]; $P < 0.024$). Thus, *P. mirabilis* urease activity is required for the increased incidence of both urolithiasis and bacteremia during coinfection but *P. stuartii* urease activity is dispensable.

Coinfection induces a proinflammatory innate immune response. The increased incidence of bacteremia during coinfection without a corresponding increase in bacterial burden suggests a role for the host immune response and, possibly, tissue destruction in promoting dissemination to the bloodstream. Macrophages and neutrophils are critical components of the host innate immune response to UTI (22–25). During UTI, macrophages and uroepithelial cells produce proinflammatory cytokines and chemokines (including the murine interleukin-8 [IL-8] functional homologs CXCL1/keratinocyte-derived chemokine and CXCL5, also known as the lipopolysaccharide-inducible CXC chemokine (LIX), CCL2/monocyte chemoattractant protein 1, CCL5/RANTES, tumor necrosis factor alpha [TNF-α], interferon [IFN], IL-1β, IL-6, IL-10, and IL-17) that attract neutrophils to the site of infection and regulate antibacterial defenses (23, 26–29). To determine if the magnitude of the innate immune response during coinfection differs from that during single-species infection, urine samples were collected at 6, 24, 48, 72, and 96 hpi and a multiplexed bead-based flow cytometry assay was used to quantify 11 cytokines and chemokines in each sample (Fig. 4).

Overall, single-species infection with *P. stuartii* resulted in minimal inflammation which was not significantly different from that achieved with mock inoculation with phosphate-buffered saline (PBS) at any time point. Compared with the response elicited by infection with *P. stuartii* or mock inoculation, single-species infection with *P. mirabilis* elicited a moderate response, with significantly more CXCL1 being produced at 72 hpi, larger amounts of IL-10 being produced at 6 and 96 hpi, and a trend toward increased amounts of IFN-γ being produced at 48 hpi. The most striking difference, however, was the potent proinflammatory response elicited by coinfection with *P. mirabilis* and *P. stuartii* at 48 hpi, which was significantly higher than that for all other infection groups for CCL2, CCL5, CXCL1, IL-6, IL-10, IL-17A, TNF-α, beta interferon (IFN-β), and IFN-γ. Coinfection therefore elicits a significantly more potent proinflammatory innate immune response than single-species infection, particularly at 48 hpi, when the peak urine pH is achieved.

Enhanced urease activity contributes to tissue damage and inflammation. As urease-mediated alkalinization of urine can cause direct damage to renal tissue (30) and induction of a potent innate immune response may lead to tissue destruction, we hypothesized that the enhanced urease activity that occurs during *P. mirabilis* and *P. stuartii* coinfection may directly promote dissemination to the bloodstream by causing greater damage to bladder and kidney tissue. Indeed, in a bivariable logistic regression model, a urine pH of 8 or higher at any point on days 1 to 4 postinoculation was significantly associated with the development of bacteremia (OR = 3.0 [95% CI = 1.2 to 7.7]; $P < 0.019$). Importantly, this association remained significant after adjustment of the model for infection type (single-species infection versus coinfection; adjusted OR [aOR] = 2.8 [95% CI = 1.1 to 7.1]; $P < 0.035$). As expected, a urine pH of 8 or higher was also associated with the development of urolithiasis (OR = 10.4 [95% CI = 2.8 to 38.6]; $P < 0.001$).

TABLE 1 Incidence of severe disease following single-species or polymicrobial infection in a murine model of ascending UTI

Parameter	No. (%) of mice[e]										
	Single-species infections					Coinfections					
	P. mirabilis ($n = 20$)	*P. mirabilis* Δ*ure* ($n = 11$)	*P. stuartii* ($n = 21$)	*P. stuartii* Δ*ure* ($n = 17$)	Total ($n = 69$)	*P. mirabilis* + *P. stuartii* ($n = 23$)	*P. mirabilis* + *P. stuartii* Δ*ure* ($n = 17$)	*P. stuartii* + *P. mirabilis* Δ*ure* ($n = 12$)	*P. mirabilis* Δ*ure* + *P. stuartii* Δ*ure* ($n = 12$)	Total ($n = 64$)	Total for all infections ($n = 133$)
Urine pH 8[a]	7 (35)	0 (0)	0 (0)	0 (0)	7 (10)	11 (48)	3 (18)	0 (0)	0 (0)	14 (22)	21 (16)
Urolithiasis[b]	1 (5)	0 (0)	1 (5)	0 (0)	2 (3)	8 (35)	3 (18)	0 (0)	0 (0)	11 (17)	13 (10)
Tissue damage[c]	8 (40)	0 (0)	6 (29)	2 (12)	16 (23)	16 (70)***	5 (29)***	3 (25)	0 (0)	24 (38)	40 (30)
Bacteremia[d]	6 (30)	2 (18)	4 (19)	2 (12)	14 (20)	12 (52)*	10 (59)*	3 (25)	4 (33)	29 (45)*	43 (32)

[a]Urine pH measurement of 8 or higher at any time postinoculation.
[b]Assessed by gross macroscopic examination of bladder and kidneys upon euthanasia.
[c]A combined histopathology score (cystitis plus pyelonephritis) of 4 or greater is indicative of moderate to severe tissue damage.
[d]Assessed by spleen colonization.
[e]*, $P < 0.05$; ***, $P < 0.001$. *P* values were determined by logistic regression.

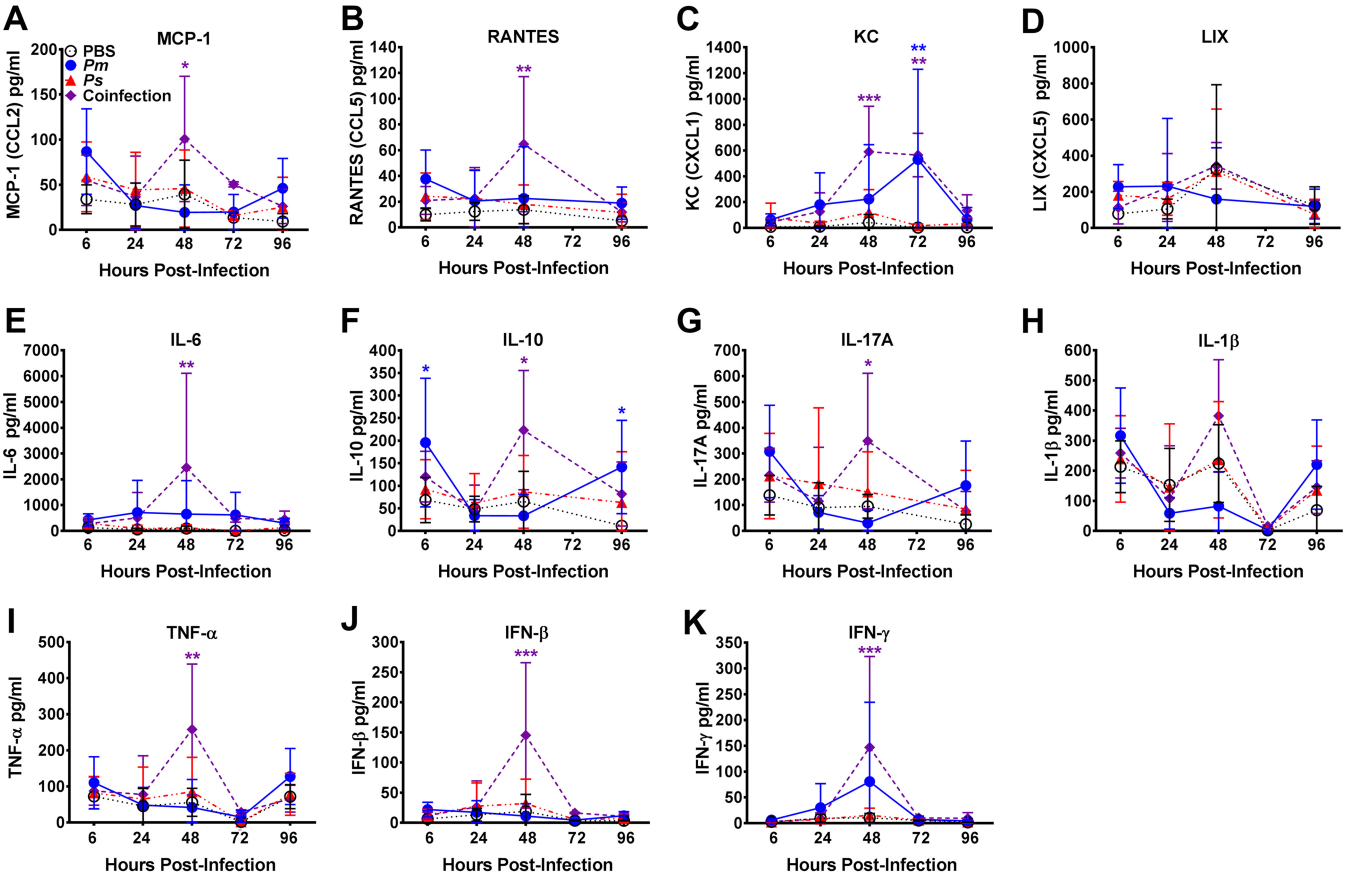

FIG 4 Coinfection promotes a proinflammatory innate immune response. CBA/J mice were inoculated transurethrally with 50 μl of PBS, 50 μl of 2×10^8 CFU/ml (1×10^7 CFU/mouse) of *P. mirabilis* or *P. stuartii* alone, or 50 μl of a 1:1 mixture of both species containing a total of 2×10^8 CFU/ml (1×10^7 CFU/mouse), and urine was collected to quantify the innate immune response. (A) CCL2 (monocyte chemoattractant protein 1 [MCP-1]); (B) CCL5 (RANTES); (C) CXCL1 (keratinocyte-derived chemokine [KC]); (D) CXCL5 (LIX); (E) IL-6; (F) IL-10; (G) IL-17A; (H) IL-1β; (I) TNF-α; (J) IFN-β; (K) IFN-γ. Error bars represent means $\pm$ SDs for five mice per infection group. *P* values were determined by two-way ANOVA with a *post hoc* test for significance *, $P < 0.05$; **, $P < 0.01$; ***, $P < 0.001$. Purple asterisks, significantly higher levels for coinfected mice than for mice in all other groups at a particular time point; blue stars, significantly higher levels for mice infected with *P. mirabilis* than for mice infected with *P. stuartii* or mock-infected mice.

We first sought to determine the contribution of urease activity to *P. mirabilis* and *P. stuartii* cytotoxicity *in vitro*, as measured by determination of the amount of lactate dehydrogenase (LDH) released from HEK293 cells (Fig. 5). *P. mirabilis* single-species cultures were more cytotoxic than *P. stuartii* single-species cultures, and urease activity was dispensable for *in vitro* cytotoxicity. Interestingly, coculture of *P. mirabilis* with *P. stuartii* resulted in a urease-independent enhancement of cytotoxicity over the expected level of cytotoxicity (on the basis of the proportion of each species present in the coculture and the cytotoxicity of each respective single-species culture). Thus, coculture of *P. mirabilis* and *P. stuartii* promotes increased virulence and cell damage and may lead to increased tissue damage during experimental infection when urease activity is also enhanced.

To determine if coinfection increases tissue damage, two previously developed scoring systems (31–34) were adapted to assess bladder and kidney inflammation and tissue damage for each infection group (Table S1 and Fig. S2 to S4). In agreement with the cytotoxicity results, a blind histologic examination of bladder sections revealed significantly higher cystitis scores for mice coinfected with WT *P. mirabilis* and *P. stuartii* than mice infected with *P. stuartii* alone and higher median scores for mice coinfected with WT *P. mirabilis* and *P. stuartii* than mice infected with *P. stuartii* alone (Fig. 6A). Coinfections that had enhanced urease activity *in vitro* (WT *P. mirabilis* with WT *P. stuartii* and WT *P. mirabilis* with *P. stuartii* Δ*ure*) were more likely to result in severe cystitis (score, 3) than the other coinfections (OR = 11.0 [95% CI = 1.3 to 92.6]; $P <$

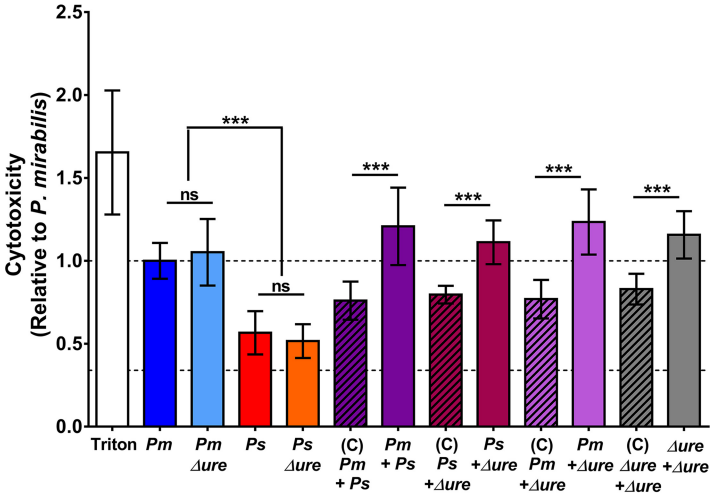

FIG 5 Cytotoxicity *in vitro* is enhanced during coculture in a urease-independent manner. The toxicity of *P. mirabilis* HI4320, *P. stuartii* BE2467, their respective urease mutants, and 1:1 mixtures of each were estimated by determination of the amount of LDH released from HEK293 cells. The level of HEK293 cell lysis under each treatment condition was normalized to the bacterial cell density of each inoculum and expressed relative to the level of treatment with WT *P. mirabilis*. The expected cytotoxicity (C; diagonal shading) of each coculture was determined on the basis of the proportion of each species present in the coculture (quantified by plating serial dilutions of the inoculum) and the cytotoxicity of each respective single-species culture. Treatment with 9% Triton X-100 was used as a positive control for maximum lysis. Dashed lines, cytotoxicity of the *P. mirabilis* single-species cultures and the background level of cytotoxicity for HEK293 cells treated with sterile urine. Error bars represent means ± SDs from three independent experiments with four technical replicates each. *P* values were determined by Student's *t* test. ***, $P < 0.001$; ns, nonsignificant.

0.027). *P. mirabilis* urease activity therefore contributes to cystitis severity during coinfection, but *P. stuartii* urease activity is not required. Although the difference was not statistically significant, infections with strains lacking urease (*P. mirabilis* Δ*ure*, *P. stuartii* Δ*ure*, or coinfection with both urease mutants) resulted in lower median cystitis scores than infections with the WT strains, suggesting that urease in general contributes to cystitis. No statistically significant differences in the pyelonephritis scores were observed between the infection groups (Fig. 6B); however, median scores were similar between mice infected with strains lacking urease and mice infected with WT strains, indicating that urease activity more strongly contributes to cystitis than pyelonephritis. This finding is in agreement with the findings of a prior study utilizing a *P. mirabilis* UreD-green fluorescent protein fusion, in which the fluorescence intensity of bacteria recovered from the bladders of infected mice was higher than that of bacteria recovered from the kidneys (35). Together, these results suggest that urease activity may be slightly dampened in the kidneys compared to the bladder during experimental ascending UTI.

To better assess the impact of enhanced urease activity on total damage within the urinary tract, a combined score was generated for each mouse by adding together the cystitis and pyelonephritis scores (Fig. 6C). Infections with strains lacking urease activity resulted in significantly lower combined scores than infections with WT strains, with the exception of infections with *P. stuartii* Δ*ure* compared to infections with WT *P. stuartii*. Furthermore, coinfections with strains with enhanced urease activity *in vitro* (WT *P. mirabilis* with WT *P. stuartii* and WT *P. mirabilis* with *P. stuartii* Δ*ure*) were more likely to cause a severe histopathology (combined score, 4, 5, or 6) than coinfections with the other groups (OR = 8.3 [95% CI = 2.3 to 30.2]; $P < 0.001$), confirming that *P. mirabilis* urease activity primarily contributes to the severity of tissue damage and inflammation during coinfection, while *P. stuartii* urease activity does not.

Damage to the renal tubule, referred to as nephrosis (36), was also analyzed to determine the contribution of enhanced urease activity during coinfection to kidney damage away from the localized site of infection (Fig. 6D). While there were no

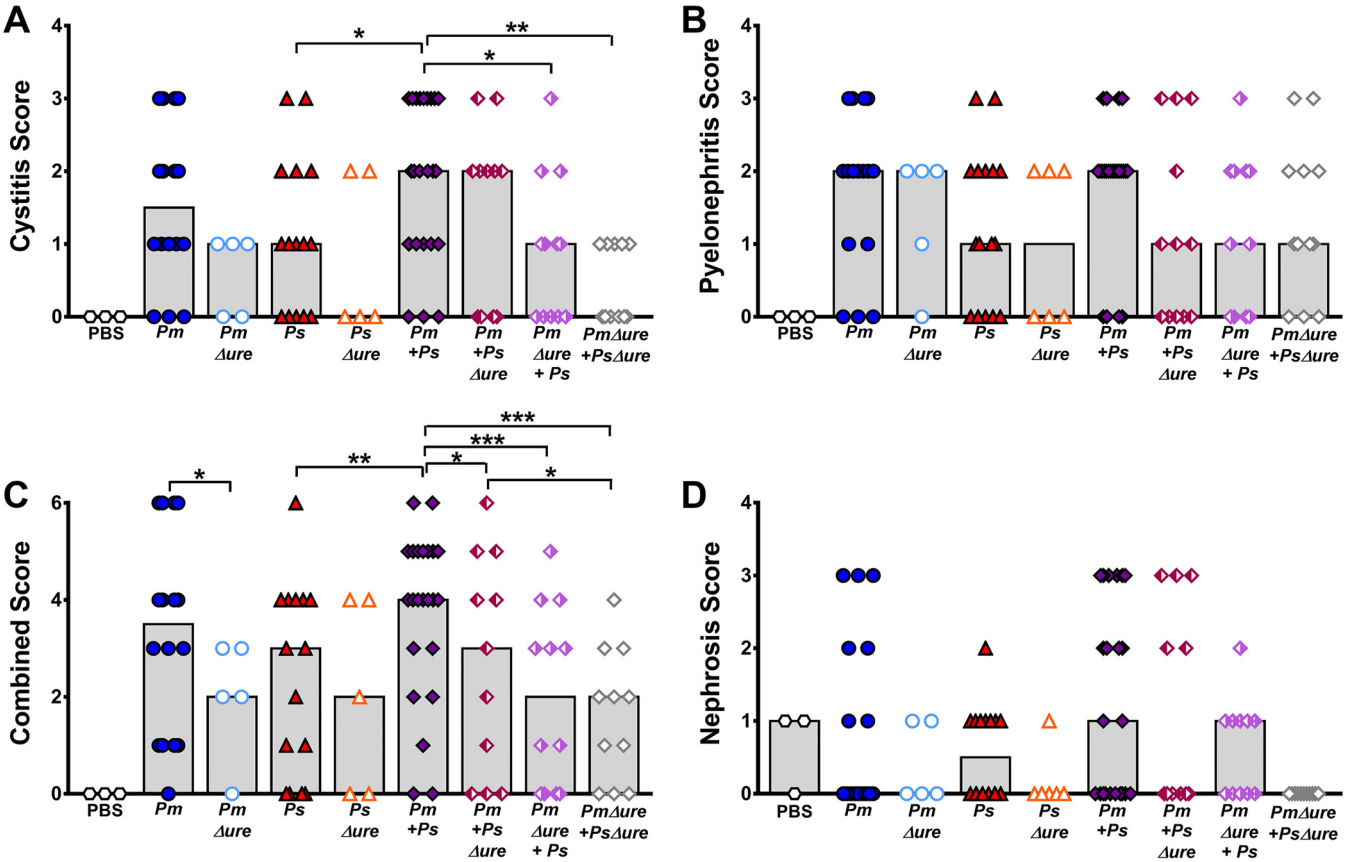

FIG 6 Enhanced urease activity during coinfection is associated with increased tissue damage and inflammation. CBA/J mice were inoculated transurethrally with 50 μl of 2×10^8 CFU/ml (1×10^7 CFU/mouse) of *P. mirabilis*, *P. stuartii*, or their respective urease mutants or coinfected with 50 μl of a 1:1 mixture of both species containing a total of 2×10^8 CFU/ml (1×10^7 CFU/mouse). Mice were sacrificed at 4 dpi, and the bladder was cut longitudinally, the left kidney was cut longitudinally, and the right kidney was cut transversely. Half of each organ was preserved in 10% formalin, embedded in paraffin, sectioned, stained with hematoxylin and eosin, and scored to determine the severity and extent of inflammation and lesions in the bladder (A) or kidney renal pelvis (B). (C) Cystitis and pyelonephritis scores were added together to generate a combined score for each individual mouse. (D) A nephrosis score for the extent of lesions and renal tubular nephrosis in the outer medulla was determined. Each symbol represents the score from one mouse; gray bars represent the median from a total of 5 to 23 mice per infection group. *P* values were determined by Student's *t* test *, $P < 0.05$; **, $P < 0.01$; ***, $P < 0.001$.

statistically significant differences between individual infection groups, histologic examination of kidney sections from coinfected mice revealed that only mice coinfected with strains with enhanced urease activity *in vitro* (WT *P. mirabilis* with WT *P. stuartii* and WT *P. mirabilis* with *P. stuartii* Δ*ure*) had severe nephrosis (score, 3). Infections with strains lacking urease activity resulted in lower median nephrosis scores overall and a greater proportion of sections negative for nephrosis compared to the results for the other infection groups, particularly for coinfection with both urease mutants.

In a bivariable logistic regression model, there was a modest association of a urine pH of 8 or higher at any point on days 1 to 4 postinoculation and cystitis (OR = 5.3 [95% CI = 1.1 to 25.0]; $P < 0.034$), and this remained significant after adjustment for infection type (aOR = 5.5 [95% CI = 1.2 to 26.2]; $P < 0.032$). Consistent with our results concerning histologic examination of kidney sections, urine pH was not associated with pyelonephritis, but achievement of a urine pH of 8 or higher at any time postinoculation was significantly associated with nephrosis (OR = 5.7 [95% CI = 1.8 to 18.0]; $P < 0.003$). This association also remained significant after adjustment for infection type (aOR = 6.0 [95% CI = 1.9 to 19.4]; $P < 0.003$). Taken together, these results indicate that urease activity contributes to cystitis and nephrosis but not pyelonephritis, and the correlation between enhanced urease activity and severe tissue damage suggests that high urease activity is likely the predominant driving factor promoting dissemination to the bloodstream, particularly during coinfection.

Enhanced urease activity promotes urolithiasis, tissue damage, and bacteremia during CAUTI. To better mimic the conditions encountered by *P. mirabilis* and *P. stuartii* in a host with an indwelling urinary catheter, a 4-mm segment of sterile silicone catheter tubing was inserted into the bladder of the mice at the time of transurethral inoculation and retained within the bladder for the 4-day course of infection. This method has been developed and tested by other groups and was shown to induce a potent proinflammatory environment within the bladder (22, 37, 38), which we recapitulated in CBA/J mice that were mock inoculated with phosphate-buffered saline (Fig. S5). The inoculum used for the catheter-associated UTI (CAUTI) model was 100-fold lower than that in the ascending UTI model to minimize discomfort to the mice and reduce the risk of bladder obstruction due to urease activity. Importantly, this decreased inoculum resulted in a similar overall bacterial burden within the catheterized urinary tract, as was observed for the higher inoculum in the ascending UTI model (compare Fig. 7 to Fig. 3).

In the CAUTI model, urease was an important fitness factor for bladder colonization by *P. mirabilis* but not for *P. stuartii*, as *P. stuartii* Δ*ure* colonized all organs to a level similar to that for the WT strain (Fig. 7B). Coinfections resulted in a bacterial burden similar to that achieved with single-species infection, consistent with our observations from the ascending UTI model. As in the ascending UTI model, a coinfection index was calculated as described previously (Fig. S1) (21). Coinfection with WT *P. stuartii* provided a modest advantage to WT *P. mirabilis* in the spleen (Fig. S1H), coinfection with *P. stuartii* Δ*ure* provided a modest advantage to WT *P. mirabilis* in the urine and spleen (Fig. S1E and H), coinfection with WT *P. stuartii* provided an advantage to *P. mirabilis* Δ*ure* in the urine, bladder, and spleen (Fig. S1A, B, and H), and coinfection with *P. stuartii* Δ*ure* provided a modest advantage to *P. mirabilis* Δ*ure* in the bladder and spleen (Fig. S1B and H). Even though the inoculum was optimized to promote a level of colonization similar to that in the ascending UTI model, there was a notable increase in the overall incidence of bacteremia in the CAUTI model compared to the ascending UTI model (78/115 mice [68%] versus 43/133 mice [32%]; Table 2). Despite this increase, coinfection further increased the likelihood of the development of bacteremia compared to that in single-species infections in a logistic regression model (OR = 2.3 [95% CI = 1.0 to 5.0]; $P < 0.048$). Mice coinfected with strains with enhanced urease activity *in vitro* (WT *P. mirabilis* with WT *P. stuartii* and WT *P. mirabilis* with *P. stuartii* Δ*ure*) again exhibited the highest incidence of urolithiasis and bacteremia. Thus, coinfection enhances disease severity in the proinflammatory environment created by an indwelling urinary catheter, and *P. mirabilis* urease remains critical for this process, while *P. stuartii* urease is still dispensable.

Histologic examination of bladder and kidney sections from the CAUTI model revealed a moderate level of baseline damage in mice mock inoculated with PBS, as expected, and similar overall trends between infection groups, as was observed in the ascending UTI model (Fig. 8). With respect to cystitis, mice coinfected with WT *P. mirabilis* and *P. stuartii* had the highest median score (Fig. 8A). In contrast to the findings obtained with the ascending UTI model, mice coinfected with strains with enhanced urease activity *in vitro* (WT *P. mirabilis* with WT *P. stuartii* and WT *P. mirabilis* with *P. stuartii* Δ*ure*) were more likely to have severe pyelonephritis (score, 3) than mice coinfected with the other groups (Fig. 8B) (OR = 13.0 [95% CI = 1.3 to 128.1]; $P < 0.028$); however, this association should be interpreted with caution due to the wide confidence interval. The combined scores appeared to further amplify this observation (Fig. 8C), with mice coinfected with strains with enhanced urease activity *in vitro* (WT *P. mirabilis* with WT *P. stuartii* and WT *P. mirabilis* with *P. stuartii* Δ*ure*) having a significantly increased likelihood of severe histopathology (combined score, 4, 5, or 6) than mice coinfected with the other groups (OR = 15.5 [95% CI = 3.3 to 72.9]; $P < 0.001$). Although the difference was not statistically significant, infections with strains lacking urease (single-species infections with *P. mirabilis* Δ*ure* or *P. stuartii* Δ*ure* or coinfection with both urease mutants) again resulted in lower median cystitis scores and combined scores than single-species infections with the WT strains, suggesting that urease in

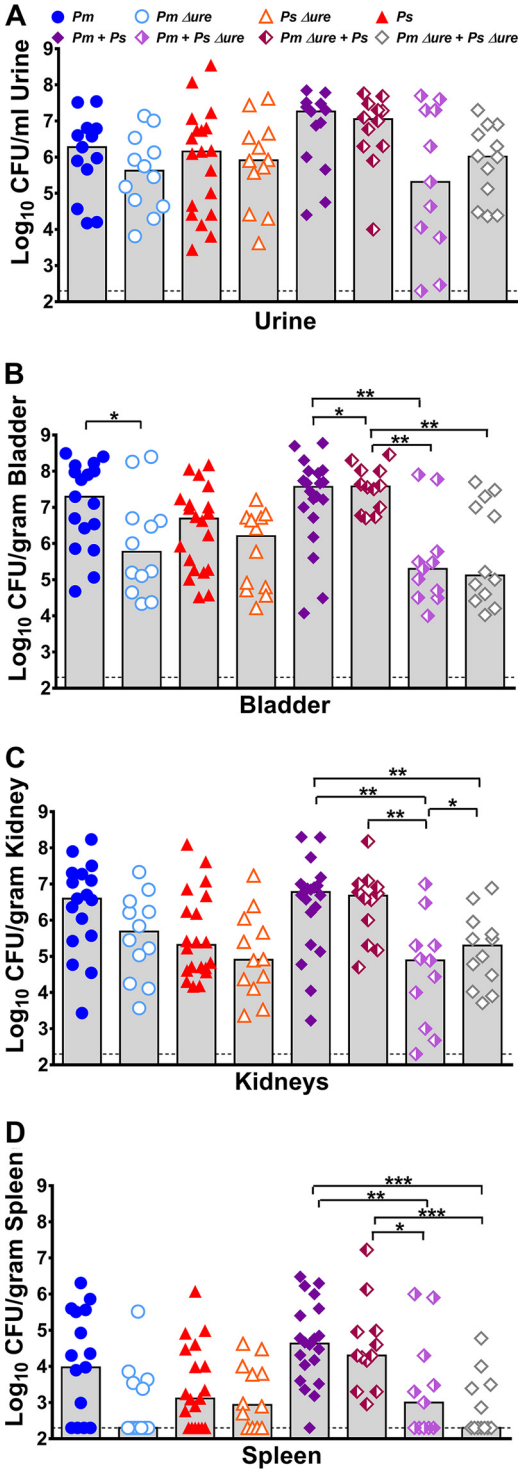

FIG 7 Enhanced urease activity during coinfection increases the incidence of bacteremia in a mouse model of CAUTI. CBA/J mice were inoculated transurethrally with 50 μl of 2×10^6 CFU/ml (1×10^5 CFU/mouse) of *P. mirabilis*, *P. stuartii*, or their respective urease mutants or coinfected with 50 μl of a 1:1 mixture of both species containing a total of 2×10^6 CFU/ml (1×10^5 CFU/mouse), and a 4-mm segment of sterile silicone tubing was inserted into the bladder during inoculation. Urine was collected, and mice were sacrificed at 4 dpi. One-half of the bladder, one-half of each kidney, and the entire spleen were homogenized and plated on LB agar to determine the bacterial burden. Each symbol represents the number of CFU per milliliter of urine (A), the number of CFU per gram of bladder tissue (B), the number of CFU per gram of kidney tissue (C), or the number of CFU per gram of spleen tissue from individual mice. Gray bars, the median from a minimum of two independent experiments with 5 to 6 mice per infection group (total number of mice, 11 to 20 per infection group); dashed lines, limit of detection. *P* values were determined by a nonparametric Mann-Whitney test. *, $P < 0.05$; **, $P < 0.01$; ***, $P < 0.001$.

TABLE 2 Incidence of severe disease following single-species or polymicrobial infection in a murine model of CAUTI

Parameter	No. (%) of mice[d]										
	Single-species infections					Coinfections					
	P. mirabilis ($n = 17$)	*P. mirabilis* Δ*ure* ($n = 12$)	*P. stuartii* ($n = 19$)	*P. stuartii* Δ*ure* ($n = 12$)	Total ($n = 60$)	*P. mirabilis* + *P. stuartii* ($n = 20$)	*P. mirabilis* + *P. stuartii* Δ*ure* ($n = 12$)	*P. stuartii* + *P. mirabilis* Δ*ure* ($n = 11$)	*P. mirabilis* Δ*ure* + *P. stuartii* Δ*ure* ($n = 12$)	Total ($n = 55$)	Total for all infections ($n = 115$)
Urolithiasis[a]	3 (18)	0 (0)	0 (0)	0 (0)	3 (5)	5 (25)	3 (25)	0 (0)	0 (0)	8 (14)	11 (10)
Tissue damage[b]	7 (35)	2 (18)	5 (24)	2 (12)	16 (23)	12 (52)***	8 (47)***	3 (25)	2 (17)	25 (39)	41 (36)
Bacteremia[c]	11 (65)	5 (42)	13 (68)	7 (58)	36 (60)	19 (95)***	12 (100)***	6 (55)	5 (42)	42 (76)*	78 (68)

[a]Assessed by gross macroscopic examination of bladder and kidneys upon euthanasia.

[b]A combined histopathology score (cystitis plus pyelonephritis) of 4 or greater is indicative of moderate to severe tissue damage.

[c]Assessed by spleen colonization.

[d]*, $P < 0.05$; ***, $P < 0.001$. *P* values were determined by logistic regression.

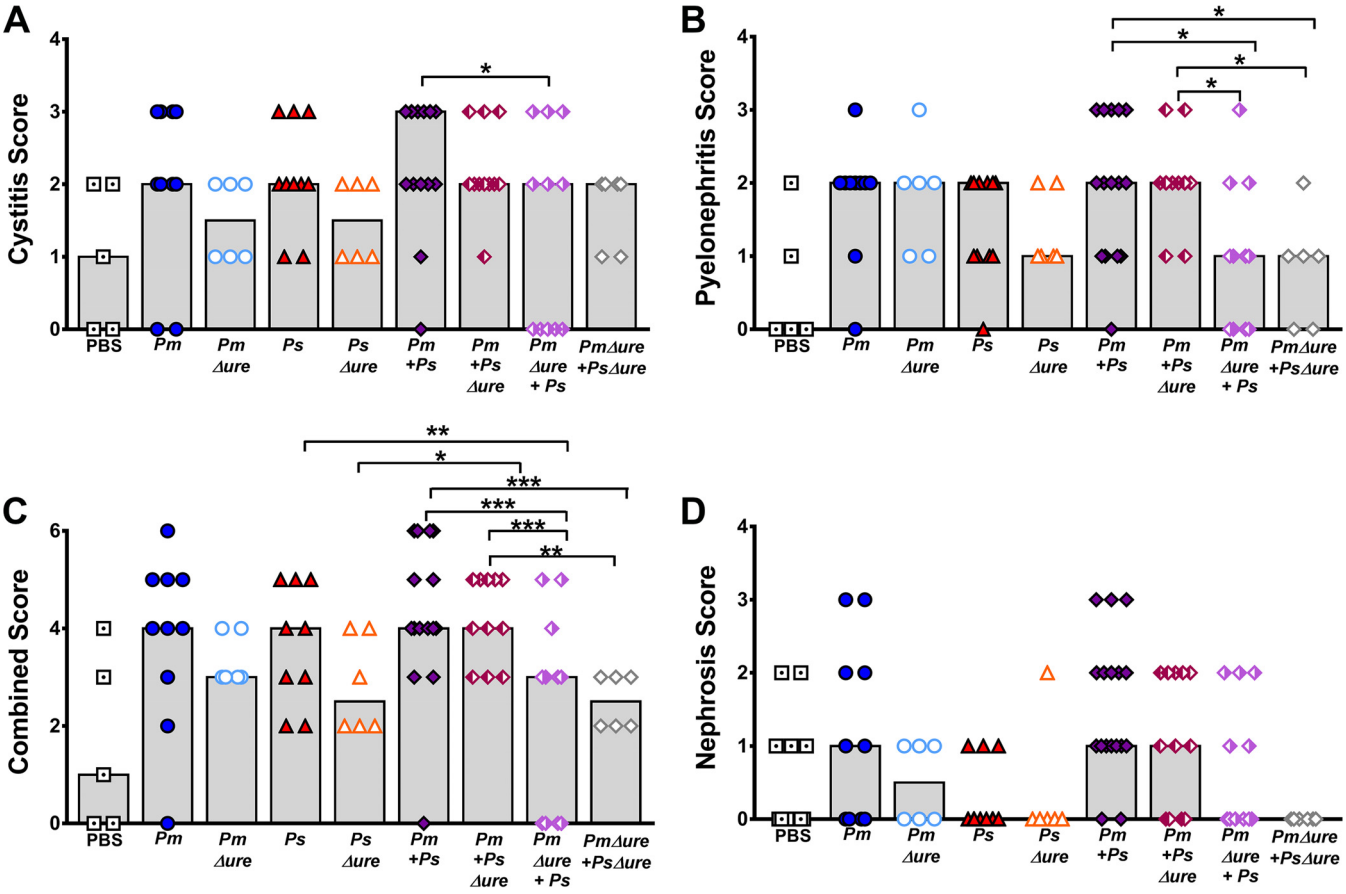

FIG 8 Enhanced urease activity during coinfection is associated with increased tissue damage and inflammation in a mouse model of CAUTI. CBA/J mice were inoculated transurethrally with 50 μl of 2×10^6 CFU/ml (1×10^5 CFU/mouse) of *P. mirabilis*, *P. stuartii*, or their respective urease mutants or coinfected with 50 μl of a 1:1 mixture of both species containing a total of 2×10^6 CFU/ml (1×10^5 CFU/mouse), and a 4-mm segment of sterile silicone tubing was inserted into the bladder during inoculation. Mice were sacrificed at 4 dpi, and the bladder was cut longitudinally, the left kidney was cut longitudinally, and the right kidney was cut transversely. Half of each organ was preserved in 10% formalin, embedded in paraffin, sectioned, stained with hematoxylin and eosin, and scored to determine the severity and extent of inflammation and lesions in the bladder (A) or kidney renal pelvis (B). (C) Cystitis and pyelonephritis scores were added together to generate a combined score for each individual mouse. (D) A nephrosis score for the extent of lesions and renal tubular nephrosis was determined. Each symbol represents the score from one mouse; gray bars represent the median for a total of 6 to 15 mice per infection group. *P* values were determined by Student's *t* test. *, $P < 0.05$; **, $P < 0.01$; ***, $P < 0.001$.

general contributes to tissue damage within the catheterized urinary tract. As in the ascending UTI model, no statistically significant differences in renal tubular nephrosis scores were observed between the infection groups (Fig. 8D). It is notable that infections with strains lacking urease again resulted in lower median nephrosis scores overall than those in the other infection groups and a greater proportion of sections negative for nephrosis than the proportion in the other infection groups, particularly for coinfection with both urease mutants. Taken together, these results indicate that urease activity has a greater influence on pyelonephritis than cystitis when a foreign body causing a high baseline level of inflammation is maintained in the bladder. We were unable to monitor the urine pH during the course of infection in the CAUTI model due to concerns about bladder blockage or obstruction and discomfort to the animals. However, the combined results of these infection studies suggest that urease activity, particularly the enhanced urease activity that occurs during coinfection, is the primary factor promoting dissemination to the bloodstream in experimental CAUTI, as in ascending UTI.

Enhanced urease activity is a widespread phenomenon. To exclude the possibility of enhanced urease activity being unique to the *P. mirabilis* and *P. stuartii* isolates used in this study (HI4320 and BE2467, respectively), we conducted coculture experiments with three additional *P. stuartii* isolates and five additional *P. mirabilis* isolates

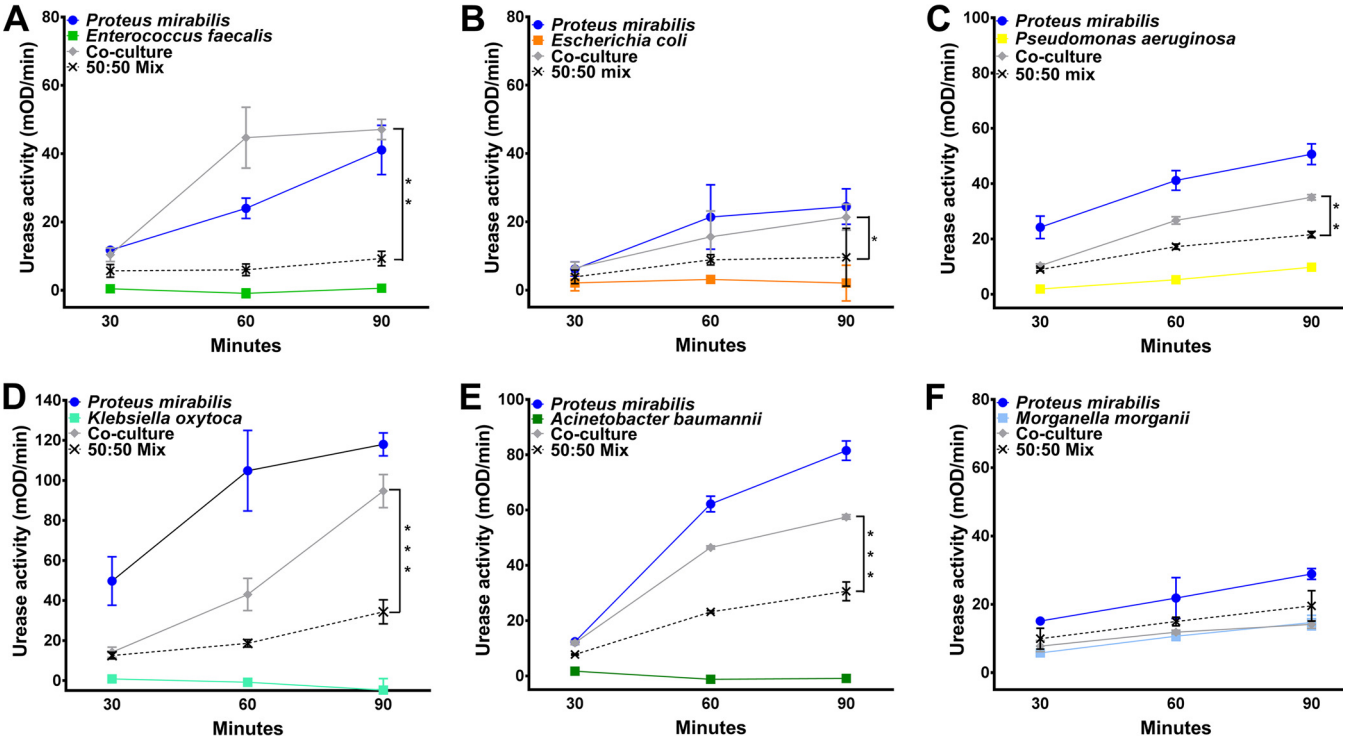

FIG 9 *P. mirabilis* urease activity is enhanced by other uropathogens. *P. mirabilis* HI4320 and a panel of uropathogens isolated from the urine of catheterized nursing home residents were cultured individually or cocultured in filter-sterilized human urine to measure urease activity. (A) Representative graph of urease activity resulting from coculture of *P. mirabilis* with *Enterococcus faecalis* compared to that resulting from a 50:50 mixture of single-species cultures at each time point ($n = 3$ isolates tested). (B) Representative graph of urease activity resulting from coculture of *P. mirabilis* with *Escherichia coli* compared to that resulting from a 50:50 mixture of single-species cultures at each time point ($n = 4$ isolates tested). (C) Representative graph of urease activity resulting from coculture of *P. mirabilis* with a urease-negative strain of *Pseudomonas aeruginosa* compared to that resulting from a 50:50 mixture of single-species cultures at each time point ($n = 3$ isolates tested). (D) Representative graph of urease activity resulting from coculture of *P. mirabilis* with a urease-negative strain of *Klebsiella oxytoca* compared to that resulting from a 50:50 mixture of single-species cultures at each time point ($n = 4$ isolates tested). (E) Representative graph of urease activity resulting from coculture of *P. mirabilis* with *Acinetobacter baumannii* compared to that resulting from a 50:50 mixture of single-species cultures at each time point ($n = 2$ isolates tested). (F) Representative graph of urease activity resulting from coculture of *P. mirabilis* with *Morganella morganii* compared to that resulting from a 50:50 mixture of single-species cultures at each time point ($n = 4$ isolates tested). Graphs are representative of those from at least two independent experiments. Error bars represent means ± SDs from at least three technical replicates. *P* values were determined by two-way ANOVA. *, $P < 0.05$; **, $P < 0.01$; ***, $P < 0.001$.

(Fig. S6). Enhanced urease activity was observed for all combinations of three out of four *P. stuartii* isolates with all six *P. mirabilis* isolates, save one (17 out of 18 combinations), and 1 out of 6 combinations involving the fourth *P. stuartii* isolate (Table S2). Using urease mutants, we determined that the *P. mirabilis* HI4320 urease was required for enhanced activity during coculture with all three *P. stuartii* isolates and the *P. stuartii* BE2467 urease was dispensable for enhancing the urease activity of all six *P. mirabilis* isolates.

We recently determined that *P. mirabilis* is the most common uropathogen in CAUTIs from Michigan nursing home residents, followed by *Enterococcus* species, *Escherichia coli*, and *Pseudomonas aeruginosa* (8). To determine if other uropathogens are capable of enhancing *P. mirabilis* urease activity, we conducted coculture experiments with both historic and recent clinical isolates from catheterized nursing home residents, including multidrug-resistant isolates and a vancomycin-resistant *Enterococcus faecalis* isolate (Fig. 9). *P. mirabilis* urease activity was enhanced to various degrees by 3/3 recent *E. faecalis* urine isolates (1 vancomycin-resistant isolate and 2 vancomycin-sensitive isolates), 3/4 *E. coli* urine isolates, 3/3 *P. aeruginosa* urine isolates, 4/4 *Klebsiella pneumoniae* urine isolates, 2/2 *Klebsiella oxytoca* urine isolates, and 2/2 *Acinetobacter baumannii* bacteremia isolates (Fig. 9A to E). It is important to note that while some *K. pneumoniae* and *P. aeruginosa* isolates are urease positive, all 6 *Klebsiella* isolates and 1/3 *P. aeruginosa* isolates were negative for urease activity in our assay. Thus, isolates that lack urease activity remain capable of enhancing *P. mirabilis* urease

activity. Curiously, *P. mirabilis* urease activity was not enhanced by the majority of *Morganella morganii* urine isolates (3 out of 4; Fig. 9F). In conclusion, the presence of other uropathogens capable of enhancing *P. mirabilis* urease activity during polymicrobial urine colonization may significantly impact the likelihood of development of severe disease, and the underlying mechanism of enhanced urease activity may represent a widespread target for decreasing the risk of complications, such as urolithiasis and bacteremia.

DISCUSSION

Urinary tract infection (UTI) is the most common health care-associated infection worldwide (1), with approximately 80% of UTIs being due to indwelling urinary catheters. Older adults are at an even higher risk for UTI and CAUTI than younger adults due to several factors, including a higher rate of asymptomatic urine colonization, functional abnormalities, chronic diseases, and certain medications (39). We recently determined that *P. mirabilis* was the most common organism in CAUTIs experienced by nursing home residents in southeast Michigan, being present in a high percentage of both single-species and dual-species infections (8), which is consistent with the findings of previous studies of catheterized individuals in long-term-care facilities (6, 7, 40). Infections with *P. mirabilis* are typically complicated by the formation of bladder and kidney stones and permanent renal damage (9, 14, 15), there are no currently available vaccines for *P. mirabilis*, and the incidence of multidrug-resistant isolates is on the rise (41). *P. mirabilis* is also a common constituent of polymicrobial CAUTI (7, 8), and there is a growing appreciation for the influence of polymicrobe-host interactions on disease severity (42, 43). It is imperative to identify novel targets for the prevention or disruption of *P. mirabilis* infection, particularly in the context of polymicrobial infection. In this study, we show that the presence of *P. stuartii* and other common uropathogens in a coinfection setting enhances *P. mirabilis* urease activity, leading to an increased pathogenic potential, including an increased severity of cystitis, pyelonephritis, nephrosis, urolithiasis, and bacteremia during experimental UTI and CAUTI. The underlying mechanism of this enhanced pathogenicity may represent a potential target for reducing the pathogenic potential of *P. mirabilis* bacteriuria.

A recent study found that *P. mirabilis* HI4320 attaches to the urothelial surface within 30 min postinoculation, and while it may invade the urothelium, it does not frequently form intracellular communities, in contrast to uropathogenic *E. coli* (44). Instead, *P. mirabilis* forms large extracellular clusters within the bladder lumen, visible as early as 10 hpi, that contain urothelial cell debris, mineral deposits, and neutrophils and are associated with urothelial destruction and early stages of urolithiasis (44). Most relevant to the present study, *P. mirabilis* urease was critical for the formation of these extracellular clusters (44). Although we did not directly assess the formation of extracellular clusters in the present study, it is likely that similar structures form during coinfection with *P. mirabilis* and *P. stuartii* in the ascending UTI model and possibly in the CAUTI model as well. The silicone catheter itself may also serve as a substrate for the initial formation of these clusters, facilitating the development of destructive and resistant bacterial populations. Our data indicate that the formation of these clusters during coinfection would result in a high local pH and increased toxin production, which would ultimately lead to an increase in tissue destruction and bacteremia during coinfection.

The increase in proinflammatory cytokines and chemokines in the urine of coinfected mice at 48 hpi provides further support for this hypothesis, as the formation of *P. mirabilis* extracellular clusters also stimulated neutrophil recruitment (44). This is particularly notable, as IL-1β levels were higher in coinfected mice than mice in the other infection groups at 48 hpi. IL-1β processing and secretion are mediated by caspase 1 activation via the NLRP3 inflammasome (45), which is potently induced by *P. mirabilis* (46) and can also be activated by uric acid crystals and other crystalline structures (47). NLRP3 may play a critical role in *P. mirabilis* pathogenesis, particularly

the tissue damage that occurs during coinfection and possibly in dissemination to the bloodstream.

While urease is clearly a virulence factor critical for the severity of coinfection, it is important to note that urease is not the only important virulence factor for *P. mirabilis* or *P. stuartii*, as their respective urease mutants were still capable of colonizing the urinary tract and causing both tissue damage and bacteremia, albeit in a lower percentage of mice than the parental isolates. Although the difference was not statistically significant, mice that were coinfected with both urease mutants had a slightly higher incidence of bacteremia than mice with single-species infections with either mutant (33% versus 14%), indicating that other urease-independent factors also likely contribute to an enhanced severity of disease during coinfection. This is further supported by our finding that coinfection of HEK293 cells resulted in greater cytotoxicity than single-species infections in a urease-independent manner. *P. mirabilis* possesses numerous additional virulence factors that contribute to colonization of the urinary tract (48), and many of these may also play a role in the increased severity of disease during coinfection. In particular, MR/P fimbriae contribute to the formation of *P. mirabilis* extracellular clusters (44), and hemolysin and *Proteus* toxic agglutinin contribute to cytotoxicity and tissue damage (31, 49). The contribution of these factors to increased disease severity during coinfection warrants exploration.

Little is known regarding *P. stuartii* virulence factors for uropathogenesis. As the urease activity of *P. stuartii* is significantly lower than that of *P. mirabilis* and the *P. stuartii* urease mutant did not exhibit a colonization defect in the CAUTI model, in which there is a high degree of baseline inflammation, it is possible that a primary function of urease in *P. stuartii* may be to promote neutrophil recruitment or induce the formation of extracellular clusters similar to those formed by *P. mirabilis*. The genome sequence of *P. stuartii* BE2467 revealed several genes with a potential role in virulence, including genes for adhesins, bacteriocins, putative toxins, and numerous metabolic pathways that may be critical for survival within the urinary tract. The contribution of specific *P. stuartii* gene products to virulence during single-species and polymicrobial infection is actively under investigation.

In addition to *P. mirabilis*, the most prevalent organisms in CAUTIs experienced by nursing home residents in southeast Michigan were *Enterococcus* species ($n = 38$ cultures [21%]), *E. coli* ($n = 37$ [20%]), and *P. aeruginosa* ($n = 34$ [19%]), while *P. stuartii* was present in only 7 urine cultures (4%) (8). It was therefore critical to test the impact of these organisms on *P. mirabilis* urease activity during coculture. A notable finding of our study was the revelation that other uropathogens can influence *P. mirabilis* urease, even when they lack urease activity themselves. In addition to the *P. stuartii* Δ*ure* mutant, recent *E. coli*, *Enterococcus faecalis*, *P. aeruginosa*, *K. pneumoniae*, and *K. oxytoca* urine isolates, including some that are naturally urease negative, also enhanced *P. mirabilis* urease activity and may similarly increase the risk of CAUTI complications. Prior work from the Mobley laboratory showed that coinfection with *E. coli* CFT073 and *P. mirabilis* HI4320 dramatically increased *E. coli* colonization out to 7 days postinoculation (dpi) (50). While spleen colonization was not addressed, *P. mirabilis* and *E. coli* coinfection may similarly increase the incidence of bacteremia. Also notable was the observation that urease-positive *M. morganii* appeared to dampen *P. mirabilis* urease activity during coculture and may be associated with a decreased risk of urolithiasis and bacteremia during polymicrobial colonization. Taken together, these observations are consistent with previous reports of catheter cocolonization frequencies and obstruction: (i) *P. mirabilis* was commonly present in catheter biofilms containing *P. stuartii*, *K. pneumoniae*, or *E. faecalis* but rarely present on catheters colonized by *M. morganii* (51); (ii) *P. mirabilis* was unable to encrust catheters precolonized by *M. morganii* (51); and (iii) *M. morganii* was more often isolated from unobstructed catheters than obstructed catheters (6).

As other organisms influence *P. mirabilis* urease activity, the presence of these organisms in catheter biofilms, for instance, may also impact disease severity and

the risk of bacteremia. If so, the underlying mechanism of enhanced urease activity may represent a novel target for limiting the detrimental consequences of catheter colonization by urease-producing bacteria. Ultimately, patient-oriented research will be necessary to determine which organisms are the most common cocolonizers of catheterized individuals and to monitor the impact of cocolonization on the progression from asymptomatic bacteriuria to symptomatic infection and the development of severe consequences, such as bacteremia. Additional ongoing research efforts are focused on elucidation of the underlying mechanism of enhanced urease activity during coculture and coinfection and identifying additional virulence factors that may be regulated by this mechanism, as well as the use of a transposon insertion site sequencing approach to identify the full arsenal of *P. mirabilis* and *P. stuartii* fitness and virulence factors during coinfection compared to single-species infections.

MATERIALS AND METHODS

Ethics statement. Bacterial species were isolated from the urine of adult human subjects following the provision of informed written consent. Urine specimen collection was performed with the approval of the University of Michigan Institutional Review Board (HUM00073813). All animal protocols were approved by the Institutional Animal Care and Use Committee (IACUC) at the University of Michigan Medical School (PRO00005052), in accordance with the Office of Laboratory Animal Welfare (OLAW) and the United States Department of Agriculture (USDA), as well as guidelines specified by the Association for Assessment and Accreditation of Laboratory Animal Care International (AAALAC Intl.). Mice were anesthetized with a weight-appropriate dose (0.1 ml for a mouse weighing 20 g) of ketamine-xylazine (80 to 120 mg/kg of body weight ketamine and 5 to 10 mg/kg xylazine) by intraperitoneal injection. Mice were euthanized by inhalant anesthetic overdose followed by vital organ removal.

Bacterial strains and growth conditions. *Proteus mirabilis* HI4320 and *Providencia stuartii* BE2467 were isolated from the urine of catheterized patients in a chronic care facility (6, 52). *P. mirabilis* Δ*ure* refers to *P. mirabilis* HI4320 lacking urease activity due to disruption of the chromosomal *ureF* gene by a transposon carrying a kanamycin resistance cassette, resulting in catalytically inactive urease (53, 54). *P. stuartii* Δ*ure* refers to *P. stuartii* BE2467 lacking the entire urease operon carried by a plasmid (see below). Additional bacterial strains utilized in urease assay experiments were isolated from the urine of catheterized patients in chronic care facilities (6, 8, 52), with the exception of *Acinetobacter baumannii* strains ATCC 17978 and AB0057. Bacteria were routinely cultured at 37°C with aeration in 5 ml LB broth (10 g/liter tryptone, 5 g/liter yeast extract, 0.5 g/liter NaCl) or on LB broth solidified with 1.5% agar. *Enterococcus faecalis* isolates were cultured in brain heart infusion (Difco) broth. *P. mirabilis* HI4320 was experimentally determined to be susceptible to <5 μg/ml kanamycin and <15 μg/ml chloramphenicol, while *P. stuartii* BE2467 was resistant to >50 μg/ml kanamycin and >50 μg/ml chloramphenicol. LB medium was supplemented with 25 μg/ml kanamycin or 20 μg/ml chloramphenicol to distinguish between species.

***P. stuartii* BE2467 whole-genome sequencing.** *P. stuartii* BE2467 was cultured in LB medium overnight at 37°C with aeration, and genomic DNA was extracted using a Qiagen DNeasy blood and tissue kit following the manufacturer's protocol. Genomic DNA was sent to the University of Michigan DNA Sequencing Core for sequencing via a Pacific Biosciences RS II+ sequencer using three SMRT (single molecule, real-time) cells. Sequencing data were uploaded onto the PacBio SMRTanalysis portal (v2.3.0) and submitted to the Hierarchical Genome Assembly Process (HGAP; version 3) protocol, which includes read filtering, preassembly, assembly, and consensus polishing (55), resulting in an assembly with 4 contigs. Using the Basic Local Alignment Search Tool (BLAST), the largest contig was determined to be the main chromosomal sequence (GenBank accession number CP017054), and two other contigs were plasmid sequences (GenBank accession numbers CP017055 and CP017056). A modular open-source assembler (AMOS) (56) was used to identify overlapping regions between the ends of each plasmid sequence and trim one end, allowing circularization. No overlap in the main chromosomal sequence was found. The cleaned sequences were submitted to the PacBio Portal Resequencing protocol, including read filtering, read mapping using basic local alignment with successive refinement (BLASR) (57), and consensus calling using the PacBio Quiver algorithm. The resulting consensus sequences were resubmitted to the resequencing protocol, boosting the consensus concordance of the assembly to 100%. The resulting consensus sequences were submitted to GenBank for annotation using the Prokaryotic Genome Annotation (PGAP) pipeline.

Generation and verification of a *P. stuartii* urease mutant. A urease-negative mutant of *P. stuartii* BE2467 was generated during construction of a transposon mutant library. In brief, a mid-log culture of *P. stuartii* BE2467 was mated with *E. coli* S17 λpir harboring a modified pSAM_Cam vector in a 2:1 donor/recipient ratio for 1 h at 37°C. The mating suspension was dispensed onto a 0.45-μm-pore-size filter disk (Millipore) and spread onto LB agar with arabinose (5 μM) to induce transposase expression. After a 2-h incubation at 37°C, the filter disk was gently washed with LB broth, and the bacterial wash suspension was spread plated onto LB agar with ampicillin (200 μg/ml) and kanamycin (25 μg/ml) and incubated for 16 h at 37°C. The resulting colonies were washed off the plate into LB broth, and the suspension was diluted and plated onto urea segregation agar (53) to identify urease-negative mutants.

Two colonies failed to produce a pink halo, indicating the loss of urease activity. One colony was subjected to biochemical testing and verified to be *P. stuartii* (mannitol fermentation negative, inositol fermentation positive, phenylalanine deaminase positive, citrate utilization positive), albeit lacking urease activity. Stepwise PCR verification of the large plasmid revealed the loss of ~10 kb, resulting in the loss of kanamycin resistance, the sucrose utilization operon, and a putative [NiFe] hydrogenase, as well as the entire urease operon. Notably, the mutant did not display a growth defect in rich or minimal medium (data not shown). For simplicity, the urease-negative isolate is designated *P. stuartii* Δ*ure* for the purposes of this study.

Urease assay. An alkalimetric screen for urease activity (58) was modified for use with whole bacterial cells. Bacterial strains were cultured in LB to mid-log phase (optical density at 600 nm [OD_{600}] = 0.5) and centrifuged to pellet the bacteria, and the bacteria were resuspended in filter-sterilized dilute human urine (adjusted to ~pH 6 using an Orion Star A111 pH meter and an Orion 8220BNWP probe from Thermo Scientific and a urine specific gravity of ~1.004 using a Schuco 5711-2020 clinical refractometer). Resuspended cultures were incubated individually at 37°C with aeration or mixed in equal proportions to generate cocultures. At 30-min intervals, 1 ml was removed from each culture and centrifuged to pellet the bacteria, and the bacteria were resuspended in a 1/10 volume of 0.9% saline. The wells of a 96-well plate containing fresh filter-sterilized human urine (~pH 6; urine specific gravity, ~1.004), 0.001% (wt/vol) phenol red, and 250 mM urea were inoculated with 20 μl of the saline resuspension. Mixtures (50:50) were generated by inoculating 10 μl of each single species in saline for comparison to cocultures. At each time point, the optical density at a 562-nm wavelength was measured using a μQuant spectrometer (BioTek) over a 5-min kinetic read. Urease activity was expressed as the mean change in the optical density (mOD) per minute, as calculated by Gen5 software (BioTek).

Mouse model of ascending UTI. Infection studies were carried out as previously described (21, 59) using a modification of the protocol of Hagberg et al. (60). Bacteria were cultured overnight in LB medium and diluted to an OD_{600} of ~0.2, and CBA/J mice (Envigo) were inoculated transurethrally with 50 μl of 2×10^8 CFU/ml (1×10^7 CFU/mouse). For coinfection experiments, mice were inoculated with 50 μl of a 1:1 mixture of both species containing a total of 2×10^8 CFU/ml (1×10^7 CFU/mouse). For each infection study, 5 to 6 mice were used per infection group, with overlapping groups being utilized in 5 independent experiments. The results of all 5 independent experiments were combined to allow comparisons between all infection groups. Urination was induced in mice by external palpation of the bladder in a gentle downward motion at 6, 24, 48, 72, and 96 h postinoculation (hpi), and urine was collected directly into a sterile microcentrifuge tube for pH measurement (using an Orion Star A111 pH meter and Orion 8220BNWP probe; Thermo Scientific) and to determine the bacterial burden by plating the urine on LB agar with or without 20 μg/ml chloramphenicol to distinguish between species. Mice were euthanized at 4 days postinoculation (dpi); and bladders, kidneys, and spleens were harvested into phosphate-buffered saline (0.128 M NaCl, 0.0027 M KCl, pH 7.4). Gross inspection of the bladders and kidneys was performed to assess urolithiasis. Tissues were homogenized using an Omni TH homogenizer (Omni International) and plated using an Autoplate 4000 spiral plater (Spiral Biotech). Colonies were enumerated with a QCount automated plate counter (Spiral Biotech).

Mouse model of CAUTI. CBA/J mice were inoculated transurethrally as described above but with two modifications: the inoculum was reduced to 50 μl of 2×10^6 CFU/ml (1×10^5 CFU/mouse), and a 4-mm segment of sterile silicone tubing (outside diameter, 0.64 mm; inside diameter, 0.30 mm; Braintree Scientific, Inc.) was carefully advanced into the bladder during inoculation as described elsewhere (22, 37, 38) and retained for the duration of the study. For each infection study, 5 to 6 mice were used per infection group, with overlapping groups being utilized in 5 independent experiments. The results of all 5 independent experiments were combined to allow comparisons between all infection groups. Mice were euthanized at 4 dpi as described above for enumeration of the bacterial burden.

Quantitation of proinflammatory response. Urine samples collected from CBA/J mice at 6, 24, 48, 72, and 96 hpi were centrifuged to pellet host cells and bacteria, and supernatants were removed and stored at −80°C until use. LEGENDplex, a custom multiplexed bead-based immunoassay (BioLegend), was used to quantify 11 mouse cytokines and chemokines (CCL2, CCL5, CXCL1, CXCL5, IL-6, IL-10, IL-17A, IL-1β, TNF-α, IFN-β, and IFN-γ) from 12 μl of urine following the manufacturer's protocol. Streptavidin-phycoerythrin (SA-PE) intensity was analyzed by use of a FACSCanto flow cytometer (Becton Dickinson), and each analyte was quantified relative to the kit standard curve using LEGENDplex software (version 7.0; BioLegend).

Cytotoxicity. The toxicity of *P. mirabilis* HI4320, *P. stuartii* BE2467, their respective urease mutants, and 1:1 mixtures of each were estimated by the lactate dehydrogenase (LDH) release cytotoxicity assay as previously described (31). Briefly, bacteria were cultured in LB medium to mid-log phase (OD_{600} = 0.5) and centrifuged to pellet the bacteria, and the bacteria were resuspended in filter-sterilized human urine to induce urease activity. Resuspended cultures were incubated for 90 min individually at 37°C with aeration or mixed in equal proportions to generate cocultures. The cultures were pelleted, washed twice, resuspended in Dulbecco modified Eagle medium without supplements to a concentration of 2×10^7 CFU/ml, and laid over a monolayer of HEK293 cells at a multiplicity of infection of approximately 100:1. After 4 h at 37°C in a 5% CO_2 atmosphere, the amount of LDH released into the supernatant was measured using a CytoToxOne homogeneous membrane integrity assay (Promega). Treatment with 9% Triton X-100 for the 4-h incubation was used as a positive control for maximum lysis, and treatment with sterile urine alone was used as a negative control. The level of HEK293 cell lysis under each treatment condition was normalized to the bacterial cell density of each inoculum and expressed relative to the level of treatment with WT *P. mirabilis*. The expected cytotoxicity (C) of each coculture was determined

on the basis of the proportion of each species present in the coculture (quantified by plating serial dilutions of the inoculum) and the cytotoxicity of each respective single-species culture.

Pathological evaluation. Following euthanasia of inoculated CBA/J mice at 4 dpi, the bladders were cut longitudinally, the left kidney was cut longitudinally, and the right kidney was cut transversely. Half of each organ was preserved in 10% formalin, embedded in paraffin, sectioned, and stained with hematoxylin and eosin. Sections were examined microscopically and scored in a blind fashion by a veterinary pathologist to determine the severity and extent of inflammation and lesions using an adaptation of two previously developed semiquantitative scoring systems (31–34). The scoring rubric is provided in Table S1 in the supplemental material, and representative images of bladder (cystitis), kidney renal pelvis (pyelonephritis), and renal tubular nephrosis for each score are provided in Fig. S2 to S4.

Statistical analysis. Significance was assessed using two-way analysis of variance (ANOVA), a nonparametric Mann-Whitney test, the Wilcoxon signed-rank test, or Student's *t* test, as indicated in the figure legends. All *P* values are two-tailed at a 95% confidence interval. ANOVA, the Mann-Whitney test, and *t* tests were performed using GraphPad Prism (version 7) software (GraphPad Software, San Diego, CA). Preliminary logistic regression models were performed using Stata/MP (version 13) software (StataCorp LP, College Station, TX) and explored infection outcomes (bacteremia and urolithiasis as binary variables and histological examination scores as ordinal variables) as a function of infection parameters (urine pH, bacterial burden, infection scheme), followed by the performance of multivariable models that combined infection parameters.

Accession number(s). The sequences of the *P. stuartii* strain BE2467 chromosome, 195,378-nucleotide plasmid, and 38,206-nucleotide plasmid have been submitted to GenBank and may be found under accession numbers CP017054, CP017055, and CP017056, respectively.

SUPPLEMENTAL MATERIAL

Supplemental material for this article may be found at https://doi.org/10.1128/IAI.00808-16.

TEXT S1, PDF file, 4.5 MB.

ACKNOWLEDGMENTS

We thank the members of the H. L. T. Mobley laboratory and the University of Michigan Department of Microbiology and Immunology for helpful comments and critiques. We also thank the leadership and health care personnel at all participating nursing homes from which urine isolates were collected and the University of Michigan Infection Prevention in Aging research group.

REFERENCES

1. Hooton TM, Bradley SF, Cardenas DD, Colgan R, Geerlings SE, Rice JC, Saint S, Schaeffer AJ, Tambayh PA, Tenke P, Nicolle LE. 2010. Diagnosis, prevention, and treatment of catheter-associated urinary tract infection in adults: 2009 international clinical practice guidelines from the Infectious Diseases Society of America. Clin Infect Dis 50:625–663. https://doi.org/10.1086/650482.
2. Nicolle LE. 2012. Urinary catheter-associated infections. Infect Dis Clin North Am 26:13–27. https://doi.org/10.1016/j.idc.2011.09.009.
3. Dudeck MA, Edwards JR, Allen-Bridson K, Gross C, Malpiedi PJ, Peterson KD, Pollock DA, Weiner LM, Sievert DM. 2015. National Healthcare Safety Network report, data summary for 2013, device-associated module. Am J Infect Control 43:206–221. https://doi.org/10.1016/j.ajic.2014.11.014.
4. Nicolle LE. 2005. Catheter-related urinary tract infection. Drugs Aging 22:627–639.
5. Jacobsen SM, Stickler DJ, Mobley HLT, Shirtliff ME. 2008. Complicated catheter-associated urinary tract infections due to *Escherichia coli* and *Proteus mirabilis*. Clin Microbiol Rev 21:26–59. https://doi.org/10.1128/CMR.00019-07.
6. Mobley HLT, Warren JW. 1987. Urease-positive bacteriuria and obstruction of long-term urinary catheters. J Clin Microbiol 25:2216–2217.
7. Warren JW, Tenney JH, Hoopes JM, Muncie HL, Anthony WC. 1982. A prospective microbiologic study of bacteriuria in patients with chronic indwelling urethral catheters. J Infect Dis 146:719–723. https://doi.org/10.1093/infdis/146.6.719.
8. Armbruster CE, Prenovost K, Mobley HLT, Mody L. 14 November 2016. How often do clinically diagnosed catheter-associated urinary tract infections in nursing home residents meet standardized criteria? J Am Geriatr Soc. https://doi.org/10.1111/jgs.14533.
9. Griffith DP, Musher DM, Itin C. 1976. Urease. The primary cause of infection-induced urinary stones. Invest Urol 13:346–350.
10. Nicholson EB, Concaugh EA, Mobley HL. 1991. *Proteus mirabilis* urease: use of a *ureA-lacZ* fusion demonstrates that induction is highly specific for urea. Infect Immun 59:3360–3365.
11. Coker C, Poore CA, Li X, Mobley HLT. 2000. Pathogenesis of *Proteus mirabilis* urinary tract infection. Microbes Infect 2:1497–1505. https://doi.org/10.1016/S1286-4579(00)01304-6.
12. Mobley HL, Island MD, Hausinger RP. 1995. Molecular biology of microbial ureases. Microbiol Rev 59:451–480.
13. Broomfield RJ, Morgan SD, Khan A, Stickler DJ. 2009. Crystalline bacterial biofilm formation on urinary catheters by urease-producing urinary tract pathogens: a simple method of control. J Med Microbiol 58:1367–1375. https://doi.org/10.1099/jmm.0.012419-0.
14. Li X, Zhao H, Lockatell CV, Drachenberg CB, Johnson DE, Mobley HLT. 2002. Visualization of *Proteus mirabilis* within the matrix of urease-induced bladder stones during experimental urinary tract infection. Infect Immun 70:389–394. https://doi.org/10.1128/IAI.70.1.389-394.2002.
15. Foxman B, Brown P. 2003. Epidemiology of urinary tract infections: transmission and risk factors, incidence, and costs. Infect Dis Clin North Am 17:227–241. https://doi.org/10.1016/S0891-5520(03)00005-9.
16. Daniels KR, Lee GC, Frei CR. 2014. Trends in catheter-associated urinary tract infections among a national cohort of hospitalized adults, 2001-2010. Am J Infect Control 42:17–22. https://doi.org/10.1016/j.ajic.2013.06.026.
17. Melzer M, Welch C. 2013. Outcomes in UK patients with hospital-acquired bacteraemia and the risk of catheter-associated urinary tract infections. Postgrad Med J 89:329–334. https://doi.org/10.1136/postgradmedj-2012-131393.
18. Rudman D, Hontanosas A, Cohen Z, Mattson DE. 1988. Clinical correlates of bacteremia in a Veterans Administration extended care facility. J Am

Geriatr Soc 36:726–732. https://doi.org/10.1111/j.1532-5415.1988.tb07175.x.
19. Watanakunakorn C, Perni SC. 1994. *Proteus mirabilis* bacteremia: a review of 176 cases during 1980-1992. Scand J Infect Dis 26:361–367. https://doi.org/10.3109/00365549409008605.
20. Kim BN, Kim NJ, Kim MN, Kim YS, Woo JH, Ryu J. 2003. Bacteraemia due to tribe Proteeae: a review of 132 cases during a decade (1991-2000). Scand J Infect Dis 35:98–103. https://doi.org/10.1080/0036554021000027015.
21. Armbruster CE, Smith SN, Yep A, Mobley HLT. 2014. Increased incidence of urolithiasis and bacteremia during *Proteus mirabilis* and *Providencia stuartii* coinfection due to synergistic induction of urease activity. J Infect Dis 209:1524–1532. https://doi.org/10.1093/infdis/jit663.
22. Guiton PS, Hung CS, Hancock LE, Caparon MG, Hultgren SJ. 2010. Enterococcal biofilm formation and virulence in an optimized murine model of foreign body-associated urinary tract infections. Infect Immun 78:4166–4175. https://doi.org/10.1128/IAI.00711-10.
23. Schiwon M, Weisheit C, Franken L, Gutweiler S, Dixit A, Meyer-Schwesinger C, Pohl JM, Maurice NJ, Thiebes S, Lorenz K, Quast T, Fuhrmann M, Baumgarten G, Lohse MJ, Opdenakker G, Bernhagen J, Bucala R, Panzer U, Kolanus W, Grone HJ, Garbi N, Kastenmuller W, Knolle PA, Kurts C, Engel DR. 2014. Crosstalk between sentinel and helper macrophages permits neutrophil migration into infected uroepithelium. Cell 156:456–468. https://doi.org/10.1016/j.cell.2014.01.006.
24. Frendeus B, Godaly G, Hang L, Karpman D, Lundstedt AC, Svanborg C. 2000. Interleukin 8 receptor deficiency confers susceptibility to acute experimental pyelonephritis and may have a human counterpart. J Exp Med 192:881–890. https://doi.org/10.1084/jem.192.6.881.
25. Haraoka M, Hang L, Frendéus B, Godaly G, Burdick M, Strieter R, Svanborg C. 1999. Neutrophil recruitment and resistance to urinary tract infection. J Infect Dis 180:1220–1229. https://doi.org/10.1086/315006.
26. Svensson M, Irjala H, Svanborg C, Godaly G. 2008. Effects of epithelial and neutrophil CXCR2 on innate immunity and resistance to kidney infection. Kidney Int 74:81–90. https://doi.org/10.1038/ki.2008.105.
27. Olszyna DP, Florquin S, Sewnath M, Branger J, Speelman P, van Deventer SJH, Strieter RM, van der Poll T. 2001. CXC chemokine receptor 2 contributes to host defense in murine urinary tract infection. J Infect Dis 184:301–307. https://doi.org/10.1086/322030.
28. Godaly G, Bergsten G, Hang L, Fischer H, Frendéus B, Lundstedt A-C, Samuelsson M, Samuelsson P, Svanborg C. 2001. Neutrophil recruitment, chemokine receptors, and resistance to mucosal infection. J Leukoc Biol 69:899–906.
29. Duell BL, Carey AJ, Tan CK, Cui X, Webb RI, Totsika M, Schembri MA, Derrington P, Irving-Rodgers H, Brooks AJ, Cripps AW, Crowley M, Ulett GC. 2012. Innate transcriptional networks activated in bladder in response to uropathogenic Escherichia coli drive diverse biological pathways and rapid synthesis of IL-10 for defense against bacterial urinary tract infection. J Immunol 188:781–792. https://doi.org/10.4049/jimmunol.1101231.
30. Musher DM, Griffith DP, Yawn D, Rossen RD. 1975. Role of urease in pyelonephritis resulting from urinary tract infection with *Proteus*. J Infect Dis 131:177–181. https://doi.org/10.1093/infdis/131.2.177.
31. Alamuri P, Eaton KA, Himpsl SD, Smith SN, Mobley HLT. 2009. Vaccination with Proteus toxic agglutinin, a hemolysin-independent cytotoxin in vivo, protects against Proteus mirabilis urinary tract infection. Infect Immun 77:632–641. https://doi.org/10.1128/IAI.01050-08.
32. Lloyd AL, Smith SN, Eaton KA, Mobley HL. 2009. Uropathogenic *Escherichia coli* suppresses the host inflammatory response via pathogenicity island genes *sisA* and *sisB*. Infect Immun 77:5322–5333. https://doi.org/10.1128/IAI.00779-09.
33. Eaton KA, Friedman DI, Francis GJ, Tyler JS, Young VB, Haeger J, Abu-Ali G, Whittam TS. 2008. Pathogenesis of renal disease due to enterohemorrhagic Escherichia coli in germ-free mice. Infect Immun 76:3054–3063. https://doi.org/10.1128/IAI.01626-07.
34. Goswami K, Chen C, Xiaoli L, Eaton KA, Dudley EG. 2015. Coculture of Escherichia coli O157:H7 with a nonpathogenic E. coli strain increases toxin production and virulence in a germfree mouse model. Infect Immun 83:4185–4193. https://doi.org/10.1128/IAI.00663-15.
35. Zhao H, Thompson RB, Lockatell V, Johnson DE, Mobley HLT. 1998. Use of green fluorescent protein to assess urease gene expression by uropathogenic *Proteus mirabilis* during experimental ascending urinary tract infection. Infect Immun 66:330–335.
36. Maxie MG. 2016. Jubb, Kennedy, and Palmer's pathology of domestic animals, vol 2. Elsevier, St. Louis, MO.
37. Kadurugamuwa JL, Modi K, Yu J, Francis KP, Purchio T, Contag PR. 2005. Noninvasive biophotonic imaging for monitoring of catheter-associated urinary tract infections and therapy in mice. Infect Immun 73:3878–3887. https://doi.org/10.1128/IAI.73.7.3878-3887.2005.
38. Kurosaka Y, Ishida Y, Yamamura E, Takase H, Otani T, Kumon H. 2001. A non-surgical rat model of foreign body-associated urinary tract infection with *Pseudomonas aeruginosa*. Microbiol Immunol 45:9–15. https://doi.org/10.1111/j.1348-0421.2001.tb01268.x.
39. Hazelett SE, Tsai M, Gareri M, Allen K. 2006. The association between indwelling urinary catheter use in the elderly and urinary tract infection in acute care. BMC Geriatr 6:15. https://doi.org/10.1186/1471-2318-6-15.
40. Breitenbucher RB. 1984. Bacterial changes in the urine samples of patients with long-term indwelling catheters. Arch Intern Med 144:1585–1588.
41. Armbruster CE, Mobley HL. 2015. *Proteus* species. *In* Yu VL (ed), Antimicrobial therapy and vaccines. Antimicrobe, Pittsburgh, PA. http://www.antimicrobe.org/b226.asp.
42. Tay WH, Chong KK, Kline KA. 2016. Polymicrobial-host interactions during infection. J Mol Biol 428:3355–3371. https://doi.org/10.1016/j.jmb.2016.05.006.
43. Rall G, Knoll LJ. 2016. Development of complex models to study co- and polymicrobial infections and diseases. PLoS Pathog 12:e1005858. https://doi.org/10.1371/journal.ppat.1005858.
44. Schaffer JN, Norsworthy AN, Sun T-T, Pearson MM. 2016. Proteus mirabilis fimbriae- and urease-dependent clusters assemble in an extracellular niche to initiate bladder stone formation. Proc Natl Acad Sci U S A 113:4494–4499. https://doi.org/10.1073/pnas.1601720113.
45. Tschopp J, Schroder K. 2010. NLRP3 inflammasome activation: the convergence of multiple signalling pathways on ROS production? Nat Rev Immunol 10:210–215. https://doi.org/10.1038/nri2725.
46. Seo SU, Kamada N, Munoz-Planillo R, Kim YG, Kim D, Koizumi Y, Hasegawa M, Himpsl SD, Browne HP, Lawley TD, Mobley HL, Inohara N, Nunez G. 2015. Distinct commensals induce interleukin-1beta via NLRP3 inflammasome in inflammatory monocytes to promote intestinal inflammation in response to injury. Immunity 42:744–755. https://doi.org/10.1016/j.immuni.2015.03.004.
47. Ciraci C, Janczy JR, Sutterwala FS, Cassel SL. 2012. Control of innate and adaptive immunity by the inflammasome. Microbes Infect 14:1263–1270. https://doi.org/10.1016/j.micinf.2012.07.007.
48. Armbruster CE, Mobley HLT. 2012. Merging mythology and morphology: the multifaceted lifestyle of *Proteus mirabilis*. Nat Rev Microbiol 10:743–754. https://doi.org/10.1038/nrmicro2890.
49. Alamuri P, Mobley HLT. 2008. A novel autotransporter of uropathogenic *Proteus mirabilis* is both a cytotoxin and an agglutinin. Mol Microbiol 68:997–1017. https://doi.org/10.1111/j.1365-2958.2008.06199.x.
50. Alteri CJ, Himpsl SD, Mobley HL. 2015. Preferential use of central metabolism in vivo reveals a nutritional basis for polymicrobial infection. PLoS Pathog 11:e1004601. https://doi.org/10.1371/journal.ppat.1004601.
51. Macleod SM, Stickler DJ. 2007. Species interactions in mixed-community crystalline biofilms on urinary catheters. J Med Microbiol 56:1549–1557. https://doi.org/10.1099/jmm.0.47395-0.
52. Mobley HL, Chippendale GR, Fraiman MH, Tenney JH, Warren JW. 1985. Variable phenotypes of *Providencia stuartii* due to plasmid-encoded traits. J Clin Microbiol 22:851–853.
53. Burall LS, Harro JM, Li X, Lockatell CV, Himpsl SD, Hebel JR, Johnson DE, Mobley HLT. 2004. *Proteus mirabilis* genes that contribute to pathogenesis of urinary tract infection: identification of 25 signature-tagged mutants attenuated at least 100-fold. Infect Immun 72:2922–2938. https://doi.org/10.1128/IAI.72.5.2922-2938.2004.
54. Island MD, Mobley HL. 1995. *Proteus mirabilis* urease: operon fusion and linker insertion analysis of *ure* gene organization, regulation, and function. J Bacteriol 177:5653–5660. https://doi.org/10.1128/jb.177.19.5653-5660.1995.
55. Chin CS, Alexander DH, Marks P, Klammer AA, Drake J, Heiner C, Clum A, Copeland A, Huddleston J, Eichler EE, Turner SW, Korlach J. 2013. Nonhybrid, finished microbial genome assemblies from long-read SMRT sequencing data. Nat Methods 10:563–569. https://doi.org/10.1038/nmeth.2474.
56. Treangen TJ, Sommer DD, Angly FE, Koren S, Pop M. 2011. Next generation sequence assembly with AMOS. Curr Protoc Bioinformatics Chapter 11:Unit 11.18. https://doi.org/10.1002/0471250953.bi1108s33.
57. Chaisson MJ, Tesler G. 2012. Mapping single molecule sequencing reads

using basic local alignment with successive refinement (BLASR): application and theory. BMC Bioinformatics 13:238. https://doi.org/10.1186/1471-2105-13-238.
58. Hamilton-Miller JM, Gargan RA. 1979. Rapid screening for urease inhibitors. Invest Urol 16:327–328.
59. Johnson DE, Lockatell CV, Hall-Craigs M, Mobley HL, Warren JW. 1987. Uropathogenicity in rats and mice of *Providencia stuartii* from long-term catheterized patients. J Urol 138:632–635.
60. Hagberg L, Engberg I, Freter R, Lam J, Olling S, Svanborg Eden C. 1983. Ascending, unobstructed urinary tract infection in mice caused by pyelonephritogenic *Escherichia coli* of human origin. Infect Immun 40:273–283.